Dual α-globin and truncated EPO receptor knockin restores hemoglobin production in α-thalassemia-derived red blood cells

Simon N. Chu[1,2,3], Eric Soupene[4], Beeke Wienert[5,] Han Yin[1,3], Devesh Sharma[1,2], Travis McCreary[1,2], Kun Jia[1,2], Shota Homma[6], Jessica P. Hampton[7], James M. Gardner[1,3], Bruce R. Conklin[5,8], Tippi C. MacKenzie[1,2], Matthew H. Porteus[7], & M. Kyle Cromer[1,2,9†]

[1]Department of Surgery, University of California, San Francisco, San Francisco, CA.
[2]Eli & Edythe Broad Center for Regeneration Medicine, University of California, San Francisco, San Francisco, CA.
[3]Diabetes Center, University of California, San Francisco, San Francisco, CA.
[4]Department of Pediatrics, University of California, San Francisco, Oakland, CA.
[5]Gladstone Institutes, San Francisco, CA.
[6]Department of Genetics, Stanford University, Stanford, CA.
[7]Department of Pediatrics, Stanford University, Stanford, CA.
[8]Department of Medicine, University of California, San Francisco, San Francisco, CA
[9]Department of Bioengineering & Therapeutic Sciences, University of California, San Francisco, San Francisco, CA.

[†]Correspondence: kyle.cromer@uscf.edu

23 **Graphical abstract**

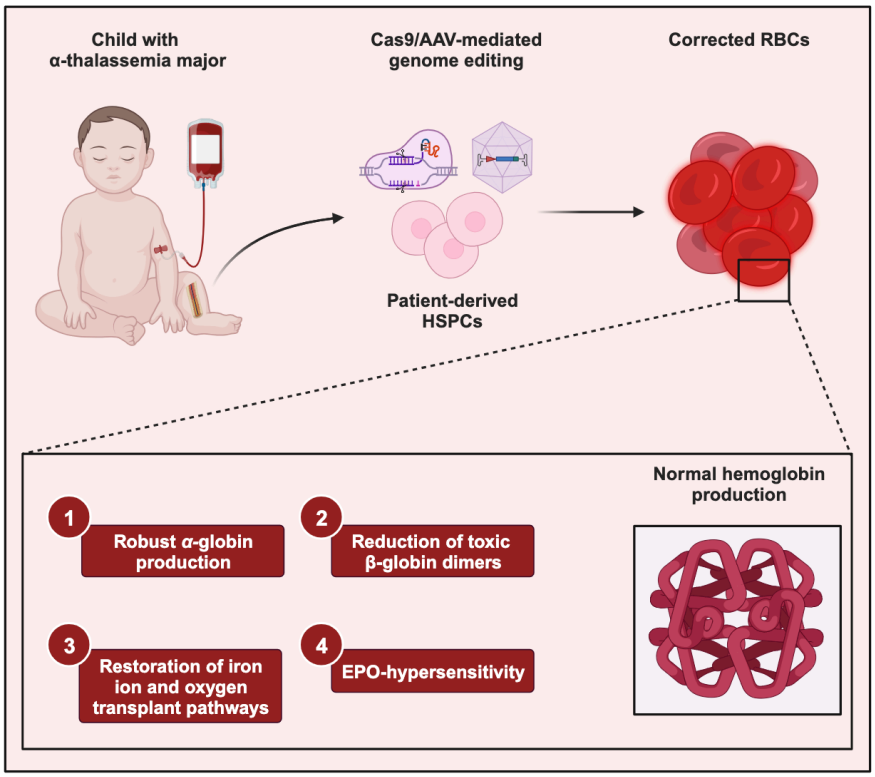

Abstract

Alpha-thalassemia is an autosomal recessive disease with increasing worldwide prevalence. The molecular basis is due to mutation or deletion of one or more duplicated α-globin genes, and disease severity is directly related to the number of allelic copies compromised. The most severe form, α-thalassemia major (αTM), results from loss of all four copies of α-globin and has historically resulted in fatality *in utero*. However, *in utero* transfusions now enable survival to birth. Postnatally, patients face challenges similar to β-thalassemia, including severe anemia and erythrotoxicity due to imbalance of β-globin and α-globin chains. While curative, hematopoietic stem cell transplantation (HSCT) is limited by donor availability and potential transplant-related complications. Despite progress in genome editing treatments for β-thalassemia, there is no analogous curative option for patients suffering from α-thalassemia. To address this, we designed a novel Cas9/AAV6-mediated genome editing strategy that integrates a functional α-globin gene into the β-globin locus in αTM patient-derived hematopoietic stem and progenitor cells (HSPCs). Incorporation of a truncated erythropoietin receptor transgene into the α-globin integration cassette dramatically increased erythropoietic output from edited HSPCs and led to the most robust production of α-globin, and consequently normal hemoglobin. By directing edited HSPCs toward increased production of clinically relevant RBCs instead of other divergent cell types, this approach has the potential to mitigate the limitations of traditional HSCT for the hemoglobinopathies, including low genome editing and low engraftment rates. These findings support development of a definitive *ex vivo* autologous genome editing strategy that may be curative for α-thalassemia.

Introduction

Alpha-thalassemia is one of the most common monogenic diseases in the world. It is currently estimated that 5% of the world's population harbors an α-thalassemia variant[1]. While the carrier frequency is highest in those with Southeast Asian heritage, data suggests that these rates are rising due to population growth, human migration, and advances in treating milder forms of the disease[2]. Humans harbor four copies of α-globin genes (a direct tandem repeat on chromosome 16), and disease severity directly correlates with the number of mutated or deleted alleles. The most severe form of the disease, in which all four copies are disrupted, is called α-thalassemia major (αTM). While this disease has historically been lethal *in utero*, patients may now survive to birth after *in utero* blood transfusions, often with excellent neurologic outcomes[3,4]. Postnatally, these patients present with a disease similar to β-thalassemia, with the absence of α-globin leading to an inability to form hemoglobin heterotetramers and subsequent severe anemia. Moreover, the accumulation of orphan β-globin chains, which form oxidized, covalently linked dimers and an unstable homotetramer (Hemoglobin H), leads to erythrotoxicity and hemolysis[5]. As a consequence, these patients require chronic transfusions, which often results in iron overload and need for iron chelation therapy[6]. Although allogeneic-hematopoietic stem cell transplantation (HSCT) may provide a cure, suitable matched donors are only available in a minority of cases and carry a risk of immune rejection and graft-versus-host-disease (GvHD)[7]. Furthermore, while numerous gene therapy and genome editing strategies have been developed for patients with β-thalassemia[8,9,10] there are no such therapies for the most severe forms of α-thalassemia, indicating a major unmet medical need for this patient population.

In this work, we developed a novel Cas9/AAV6-mediated genome editing strategy to integrate a functional copy of the *α-globin* gene into the *β-globin* locus in αTM patient-derived hematopoietic stem and progenitor cells (HSPCs) as a universal treatment strategy for the disorder—an approach that could be curative for any αTM patient regardless of the specific causative mutations or deletions. This approach allows both correction of the underlying disease as well as restoration of the β-globin:α-globin imbalance by placing the *α-globin* transgene under erythroid-specific expression of the *β-globin* locus. Taking a cue from human genetics, we also incorporated a naturally occurring truncated erythropoietin receptor (*tEPOR*) cDNA into the *α-globin* integration cassette, allowing for simultaneous correction of α-thalassemia and increased erythropoietic output from edited HSPCs[12]. By directing edited HSPCs toward increased production of clinically relevant RBCs instead of other divergent cell types, this approach has the potential to overcome many of the clinical challenges of HSCT for treatment of the hemoglobinopathies, including low editing and engraftment rates, as well as high morbidity from

83 prerequisite myeloablative regimens[13,14,15]. Similar to our prior work with β-thalassemia[8], this
84 strategy could be used in to develop an autologous-HSCT treatment for αTM, overcoming the
85 shortage of matched donors and ameliorating the risk of immune rejection and GvHD for patients
86 suffering from this disease.
87
88 **Results**
89 ***Efficient cleavage with HBB intron-targeting gRNAs***
90 Due to the high editing frequencies achieved in primary HSPCs in prior work[8,16], we sought to use
91 a Cas9/AAV6-mediated genome editing strategy to knock an *α-globin* (*HBA*) transgene into the
92 *β-globin* (*HBB*) locus in patient-derived HSPCs. To do so, we first designed and screened Cas9
93 gRNAs at the *HBB* locus. So that cleavage alone without homology-directed repair (HDR) would
94 not disrupt β-globin production, we chose 22 candidate gRNAs located in intron 1 or intron 2 as
95 well as the 3' UTR (Figure 1A and Supplemental Table 1). To determine cleavage frequencies,
96 we delivered candidate gRNAs pre-complexed with Cas9 protein to the human HUDEP-2 cell line
97 via electroporation[17]. Genomic DNA was harvested several days post-targeting and subjected to
98 PCR amplification of the region surrounding the expected cleavage site. Insertion and deletion
99 (indel) frequencies of the corresponding Sanger sequences were then quantified using ICE
100 analysis[18]. We found that targeting the 5' and 3' UTR regions of *HBB* proved not to be feasible,
101 as the former had significant homology to δ-globin and the latter had no gRNAs with detectable
102 cleavage. We found that the most efficient gRNAs corresponded to sg7 in intron 1, and to sg11
103 and 13 in intron 2 (Figure 1A and Supplemental Figure 1)[19]. *In silico* off-target analysis of these
104 guides using COSMID[20,21] revealed that sg7 had the most favorable predicted off-target profile
105 (Figure 1B). On further evaluation of the 19 predicted off-target sites for sg7, all were found to
106 reside in non-coding regions of the genome (Figure 1C).
107
108 ***Efficient integration of HDR templates at HBB locus***
109 Following identification of effective *HBB* intron-targeting gRNAs, we developed DNA repair
110 templates packaged in AAV6 delivery vectors that could effectively mediate HDR at these
111 cleavage sites (termed Intron 1 and Intron 2 donors; Figure 1D). Each integration cassette was
112 comprised of a SFFV promoter driving expression of a GFP reporter to allow rapid readout of
113 integration frequencies via flow cytometry. While the right homology arm of each DNA repair
114 template corresponded to the ~900bp immediately downstream of the intron 1 or intron 2 Cas9
115 cut site, the left homology arm was split away from the cleavage sites to correspond to the ~900bp
116 immediately upstream of the start codon of the endogenous *HBB* gene. As in a prior study[8], this

117 split homology arm strategy is expected to allow promoterless integration cassettes—ultimately
118 an *α-globin* transgene in this work—to be driven by the regulatory machinery of the endogenous
119 locus.
120 Once DNA repair templates were assembled and packaged into AAV6 vectors, we tested
121 each integration strategy by delivering the most effective gRNAs (sg7, 11, or 13) complexed with
122 high-fidelity Cas9 protein[22] to wild-type (WT) human primary $CD34^+$-enriched HSPCs via
123 electroporation. immediately following electroporation, we transduced cells with AAV6 vectors
124 corresponding to either intron 1 or intron 2 integration schemes. Five days later, we analyzed
125 targeting frequencies by flow cytometry (Figure 1E and Supplemental Figure 2A) and found that
126 the Intron 1 integration strategy was significantly more efficient (median of 17.1% GFP^+ cells)
127 compared to Intron 2 integration (median of 12.5% for sg11 and 13.3% for sg13; $p<0.05$) (Figure
128 1F), perhaps due to the shorter distance that the left homology arm was split away from the Cas9
129 cleavage site. In addition, both integration strategies yielded a high mean fluorescence intensity
130 (MFI) per edited cell (Figure 1G). Given the high cleavage and integration frequency, as well as
131 the favorable off-target profile of sg7, we proceeded with further testing in primary WT HSPCs
132 using the Intron 1 integration strategy.
133
134 ***Integration at HBB drives erythroid-specific expression of transgenes***
135 A key goal of this work is to achieve erythroid-specific expression of an *α-globin* transgene. To
136 test whether the *HBB* Intron 1 integration strategy is able to achieve this, we designed custom
137 promoterless integration cassettes which included either the full-length *HBA1* or *HBA2* transgene
138 (i.e., including all UTRs, exons, and introns) linked to a T2A-YFP reporter to allow quantification
139 of HDR frequency by flow cytometry and to serve as a surrogate for α-globin protein production
140 (Figure 2A). Because the specific UTRs flanking an integrated transgene can have a great bearing
141 on expression[8], we also designed integration strategies that would allow our *HBA* transgene to
142 be flanked by *HBB*, *HBA1*, and *HBA2* 5' and 3' UTRs.
143 To determine whether integration of these promoterless *α-globin* cassettes at *HBB* yielded
144 erythroid-specific expression, we edited WT HSPCs using electroporation-mediated delivery of
145 Cas9:sg7 RNP followed by transduction with AAV6 vectors containing each repair template. We
146 then performed an established, 14-day erythroid differentiation protocol[23] and quantified YFP
147 expression and RBC differentiation (staining with antibodies for CD34, CD45, CD71, and GPA)
148 via flow cytometry (Figure 2B and Supplemental Figure 2B). We found that all conditions efficiently
149 differentiated into erythroid cells (Figure 2C). However, we did observe differences among the
150 integration vectors in terms of HDR frequency and MFI of edited cells. We found that the vector

151 integrating the *HBA1* transgene and *HBA1* UTRs achieved the most highly HDR-edited population
152 of RBCs (median of 63% YFP^+ cells; Figure 2D) and the second highest MFI of the HDR-edited
153 cell population (Figure 2E). As confirmation that these integration strategies achieved erythroid-
154 specific transgene expression, we observed high YFP fluorescence in cells that acquired RBC
155 markers ($CD71^+/GPA^+$) in all editing conditions but no fluorescence above background in cells
156 retaining HSPC markers ($CD34^+/CD45^+$) (Figure 2F). We also tracked differentiation and YFP
157 expression kinetics and found that all editing conditions proceed through RBC differentiation at a
158 similar rate (Figure 2G). When monitoring expression of fluorescent reporters, we find that cells
159 edited with the constitutive SFFV-GFP integration vector maintain high expression over the
160 course of RBC differentiation, whereas all three conditions edited with HBA-2A-YFP constructs
161 display increasing fluorescence that dovetails with RBC differentiation (Figure 2H). Collectively,
162 these results indicate that integration of the *HBA* transgene at *HBB* achieves high levels of
163 erythroid-specific transgene expression.
164
165 ***α-globin integration in*** αTM ***HSPCs yields low levels of hemoglobin***
166 While T2A-YFP reporters allow rapid readout of HDR-editing frequency, to generate clinically
167 relevant constructs we created *HBA1* integration vectors without T2A-YFP that were flanked by
168 either *HBB* or *HBA1* UTRs (Figure 3A). To test these new vectors, we edited WT HSPCs as
169 before and found that both vectors mediate high frequencies of HDR editing (median of 36.6%
170 and 42.3% HDR-edited alleles for *HBB* and *HBA1* UTR vectors, respectively) as measured by a
171 custom ddPCR assay (Figure 3B).
172 We next sought to determine whether *α-globin* integration can restore hemoglobin
173 tetramer production in patient-derived HSPCs following erythroid differentiation. We isolated
174 $CD34^+$ HSPCs from a bone marrow aspirate that was taken from a ~1-year-old patient with αTM.
175 We then edited and differentiated HSPCs as before and found that all conditions were able to
176 effectively differentiate into RBCs (Figure 3C). Following ddPCR analysis, we found that cells
177 were edited at a median of 25.8% and 20.1% HDR-edited alleles for *HBB* and *HBA1* UTR vectors,
178 respectively (Figure 3D). We then performed hemoglobin tetramer HPLC analysis on edited
179 patient-derived αTM cells at the end of erythroid differentiation and found that HDR-edited cells
180 displayed a modest increase in all three alpha-containing hemoglobins (fetal hemoglobin (HbF),
181 adult hemoglobin (HbA), and hemoglobin A2 (HbA2)) compared to WT (Figure 3E-H and
182 Supplemental Figure 3). While these results demonstrate for the first time that gene therapy or
183 genome editing may be used to increase α-globin production in αTM patient-derived RBCs, it is
184 unlikely that this low level of α-globin production will yield significant clinical benefit.

185

186 ***Dual integration of α-globin and tEPOR increases hemoglobin production in*** αTM ***HSPCs***

187 Given that *α-globin* integration into *HBB* does not substantially restore hemoglobin production,
188 we sought alternative strategies to increase the therapeutic potential of this approach. As
189 described in a cohort that included an Olympic gold medalist cross-country skier[24], a premature
190 stop codon in the erythropoietin receptor (*EPOR*) was linked with a condition called congenital
191 erythrocytosis, which is characterized by non-pathogenic hyper-production of RBCs. In
192 subsequent work[12], we demonstrated that genome editing-mediated integration of a truncated
193 *EPOR* (*tEPOR)*-coding cDNA could increase erythropoietic output from primary human HSPCs.
194 Thus, we hypothesized that co-expression of *tEPOR* cDNA from our *α-globin* integration cassette
195 could lend a selective advantage to genome-edited and, therefore, α-globin-expressing erythroid
196 cells. To test this, we added a *tEPOR* cDNA at the C-terminus of the *α-globin* integration cassette
197 with expression linked by an internal ribosome entry site (Figure 4A). We then edited WT HSPCs
198 with our *HBA1*-UTRs *α-globin* integration vector from Figure 3 and compared it against the
199 bicistronic *α-globin*+*tEPOR* vector in WT HSPCs. In both instances, edited cells efficiently
200 differentiated into erythroid cells (Figure 4B). While cells edited with *α-globin* integration alone
201 maintained a constant editing rate (median of 39.2% edited alleles at d0 and 38.4% at d14), HDR
202 frequencies increased significantly over the course of erythroid differentiation in cells edited with
203 the *α-globin*+*tEPOR* cassette, rising from a median of 29.3% edited alleles at d0 to 69.9% at d14
204 (*** p=0.0004) (Figure 4C). As in prior work, this suggest that cells expressing a *tEPOR* have a
205 significant competitive advantage over unedited cells during RBC differentiation. We next tested
206 these vectors in αTM patient-derived HSPCs and again observed that edited and unedited cells
207 were able to effectively undergo erythroid differentiation (Figure 4D). As with WT cells, we found
208 that HDR-editing frequencies among cells targeted with the *α-globin* alone vector maintained a
209 consistent editing rate over the course of RBC differentiation (Figure 4E). However, we again
210 observed a dramatic increase in HDR frequencies in cells edited with the *α-globin*+*tEPOR*
211 cassette, rising from a median of 40.5% HDR-edited alleles at d4 to 60.5% at d16 (* p=0.02)**.** In
212 addition to the increase in editing frequencies, we also observed a 2-fold increase in cell counts
213 at the end of RBC differentiation in conditions edited with the *α-globin*+*tEPOR* cassette compared
214 to cells edited with the *α-globin* vector (** p=0.007) (Figure 4F), indicating that *tEPOR* expression
215 is driving increased erythropoietic output from genome-edited HSPCs.

216 To determine whether this strategy was able to restore α-globin production in the context
217 of αTM, we performed HPLC hemoglobin analysis on edited patient-derived HSPCs following
218 RBC differentiation. We found that addition of *tEPOR* to the *α-globin* integration cassette

219 dramatically increased the formation of hemoglobin tetramers, with a substantial increase in HbF,
220 HbA, and HbA2 (Figure 4G-I). Single globin chain HPLC confirmed that α-globin production was
221 indeed elevated in HDR-edited samples (Supplemental Figure 4A-B), likely driving the observed
222 increases in hemoglobin tetramer formation. We next validated these results using western blot
223 for α-globin and β-globin and found that not only do cells edited with *α-globin+tEPOR* show a
224 dramatic increase in α-globin compared to unedited and *α-globin* alone-edited patient-derived
225 RBCs, but *α-globin+tEPOR*-edited cells also show a decrease in formation of toxic β-globin
226 dimers to nearly WT levels (Figure 4J-K).
227
228 ***RNA-sequencing demonstrates restoration of oxygen transport and iron ion processes to***
229 **αTM *HSPCs***
230 We next used RNA-sequencing to reveal the transcriptional profile of αTM patient-derived HSPCs
231 edited with *α-globin* as well as *α-globin+tEPOR* integration vectors in comparison to WT unedited
232 HSPCs. Following editing and *in vitro* RBC differentiation, total RNA was isolated from edited
233 αTM patient cells as well as a healthy WT control. Bulk RNA-sequencing was then performed,
234 followed by quality control and statistical analysis (Figure 5A and Supplemental Figure 5). Total
235 normalized read counts across samples ranged from 17.6-22.0M and mapped to 17,776 unique
236 genes. The high sequence similarity between *HBA1* and *HBA2* precluded clear differentiation;
237 however, reads were exclusively assigned to one gene or another without overlap. For the *EPOR*
238 gene, the alignment was unable to differentiate the endogenous *EPOR* and our transgene *tEPOR*,
239 leading to a combined set of reads from both. In analyzing the data, we found consistent
240 expression across RBC-associated genes in both healthy control and patient-derived cells, which
241 is expected given the efficient erythroid differentiation in edited and unedited samples
242 (Supplementary Figure 6). While the most highly expressed genes by WT RBCs are the adult
243 globins (*HBA1*, *HBA2*, and *HBB*), unedited "mock" αTM RBCs expressed no detectable *HBA1* or
244 *HBA2* (Figure 5B) as expected due to confirmation of four-gene α-globin deletion in this patient.
245 When investigating the genes with the greatest rank change between WT RBCs compared to
246 αTM RBCs, it is unsurprising that the top genes are *HBA1* and *HBA2* (Figure 5C). Despite the
247 modest increase in α-globin production by *α-globin* integration alone according to HPLC, we
248 observed substantial restoration of *HBA1* and *HBA2* expression compared to mock (*HBA1* and
249 *HBA2* rising from undetectable in αTM mock to the 99.9th and 71.7th percentile of expressed
250 genes, respectively) (Figure 5B). Comparing *α-globin*-integrated αTM cells to mock, we found that
251 *HBA1* is the gene that displays the greatest rank change (Figure 5C). Predictably, this restoration
252 of *α-globin* gene expression was further amplified in cells edited with the dual the *α-globin+tEPOR*

253 vector, with *HBA1* and *HBA2* expression increasing to the 98.9th and 99.9th percentiles,
254 respectively (Figure 5B). Because this editing strategy places *tEPOR* under the strong, erythroid-
255 specific *HBB* promoter, we also found *EPOR* expression was elevated compared to all other
256 conditions. These elevated expression levels are confirmed by the fact that *HBA1*, *HBA2*, and
257 *EPOR* are among the top four genes with the greatest rank change over unedited αTM cells
258 (Figure 5C).

259 In addition, we found that *γ-globin* genes (*HBG1* and *HBG2*) were more highly expressed
260 in all αTM samples, regardless of editing, compared to the WT control (Figure 5D). This was
261 expected as the αTM HSPCs were derived from a ~1-year-old patient, whereas the WT HSPCs
262 were derived from an adult donor. Although ζ-globin is normally expressed only during the first
263 three months of gestation, we found that this gene was highly elevated in all αTM cells (among
264 the eight most highly expressed genes) compared to WT cells (Figure 5D). ζ-globin was also the
265 gene with the greatest rank change in expression in all αTM conditions compared to WT control
266 cells (Figure 5E).

267 To identify large-scale changes in biological processes, gene ontology (GO) enrichment
268 analysis was performed across the top 0.001% (eighteen) most highly expressed genes across
269 all samples. Compared to unedited mock αTM cells, *α-globin* integration alone led to enrichment
270 of various iron ion-associated pathways to levels equivalent to the WT control (Figure 5F). Further
271 improvements were observed in αTM cells edited with the dual *α-globin+tEPOR* integration
272 strategy, showing enrichment of oxygen and gas transport as well as hydrogen peroxide-
273 associated pathways to levels observed in the WT control (Figure 5F). In addition to assessing
274 GO enrichment on the most highly expressed genes within a given sample, we also performed
275 this analysis on the top 0.001% of genes with the greatest rank change across samples.
276 Unsurprisingly, we found that gas transport and gas metabolism were the most significantly
277 enriched pathways when comparing WT to unedited αTM cells (Figure 5G). When performing the
278 opposite comparison, for genes with the greatest rank change in unedited αTM vs. WT cells, we
279 found that the most significantly enriched pathways were for response to incorrect and unfolded
280 protein (Figure 5H), likely representing the cellular response to the formation of toxic β-globin
281 aggregates in the absence of α-globin. Interestingly, when comparing *α-globin+tEPOR*-edited
282 αTM cells to WT cells, we saw no significantly enriched GO pathways, indicating that this editing
283 strategy yielded cells that were not appreciably different from normal RBCs. Along with our
284 western blot data (Figure 4I), these findings suggest that while unedited αTM cells have highly
285 elevated β-globin dimers, even a modest increase in α-globin is able to mitigate the unfolded

286 protein response that occurs in the context of αTM pathology. As with WT cells, we also found no
287 significantly upregulated GO pathways when comparing *α-globin*-edited αTM cells to unedited
288 αTM cells (Alpha-thal Supplemental Data). However, when comparing *α-globin+tEPOR*-edited
289 cells to unedited αTM cells, we found a number of upregulated GO pathways, the most
290 significantly enriched being associated with cytokine-mediated signaling (likely a result of elevated
291 EPOR signaling) and hydrogen peroxide (H_2O_2) catabolism (Figure 5I).
292
293 **Discussion**
294 Given the increasing global burden of αTM and tremendous cost of disease management for
295 patients and health care systems, there is an urgent need for curative treatments for this disease.
296 To our knowledge, these results demonstrate for the first time that gene therapy or genome editing
297 may be used to restore normal hemoglobin production to αTM patient-derived RBCs. This
298 approach addresses the two major elements contributing to molecular pathology of the disease
299 in a single genome editing event: successfully increasing α-globin production as well as reducing
300 the formation of toxic β-globin dimers without noticeably disrupting β-globin formation. While the
301 cells in this work were derived from patients with four-gene-deletion αTM, our editing strategy
302 may also be effective in other transfusion-dependent phenotypes of α-thalassemia such as in
303 patients with inactivation of three α-globin genes or hemoglobin H disease[26].
304 In addition to these protein-level changes, deeper analysis reveals several interesting
305 findings at a transcriptional level. The enrichment of pathways associated with various oxidative
306 pathways in *α-globin+tEPOR*-edited cells suggest an improvement in the stability and function of
307 edited RBCs. Most notably, H_2O_2 catabolism and metabolism has been identified as a critical
308 process in preventing cellular injury in β-thalassemic erythrocytes[27], as the auto-oxidation of
309 unpaired globin chains results in the generation and release of significant amounts of superoxide
310 (O_2^-) and H_2O_2. These observations suggest that our novel genome editing strategy not only
311 restores *α-globin* gene expression, but also re-establishes essential antioxidant pathways that
312 may be critical in addressing the pathophysiology of α-thalassemia. Moreover, the high
313 expression of ζ-globin found in αTM cells hints at a possible compensatory mechanism for the
314 loss of α-globin in the cell. These findings support the hypothesis that the presence of ζ-globin in
315 patients with α-globin deletions may be protective[4,28].
316 In this work, we discovered that pairing *α-globin* transgene with a naturally occurring
317 *EPOR* variant led to the greatest restoration of α-globin production by substantially increasing
318 erythropoietic output of α-globin-expressing αTM patient-derived cells. While we observed

319 significantly higher production of adult hemoglobin tetramers from our *HBA+tEPOR* edited
320 conditions, it is clear from our HPLC analysis that fetal-to-adult hemoglobin switching is still
321 underway. Because we are knocking our transgene cassette into the *HBB* locus that is only
322 expressed later in development, we expect the results to be further amplified as hemoglobin
323 switching is completed. This method has the potential to resolve clinical challenges previously
324 encountered in HSCT for the hemoglobinopathies by lowering editing and engraftment
325 frequencies needed to correct RBC disorders. This strategy has the capacity to reduce or
326 eliminate the need for high-morbidity myeloablation currently required to clear the HSC niche,
327 which stand as a major barrier to HSCT safety and efficacy. Moreover, as patients with severe
328 anemia—such as those with αTM —have increased levels of circulating erythropoietin, a *tEPOR*-
329 based genome editing strategy may be especially potent in this context.
330 Finally, we believe this work stands as a compelling proof-of-concept. However, before
331 this editing strategy is ready for translation into patients, further preclinical studies are needed.
332 These studies include assessing the behavior of edited human αTM HSPCs after transplantation
333 into mice. This may be difficult due to the limited availability of αTM patient HSPCs given the
334 historical prenatal lethality of the disorder as well as the inability of existing mouse models to
335 effectively model human erythropoiesis *in vivo*. Nevertheless, addressing these challenges will
336 be key to paving the way for the clinical application of this promising editing strategy.
337 In summary, we present results of a comprehensive genome editing approach for the
338 treatment of α-thalassemia that restores α-globin production, reduces the formation of toxic
339 unpaired β-globin aggregates, and restores the transcriptional profile akin to that of a healthy red
340 blood cell. We believe that these findings support development of a definitive *ex vivo* autologous
341 genome editing strategy that may be curative for patients with α-thalassemia.
342
343 **Methods**:
344 ***In vitro* culture of primary HSPCs**
345 $CD34^+$ HSPCs were isolated from umbilical cord blood (provided by Stanford Binns Program) or
346 sourced from Plerixafor- and/or G-CSF-mobilized peripheral blood (AllCells and STEMCELL
347 Technologies). Bone marrow aspirates taken from patients with αTM under protocol no. 16-
348 21157, which was approved by the NHLBI Institutional Review Board. Patients provided informed
349 consent and samples were de-identified after collection. $CD34^+$ HSPCs were isolated using a
350 EasySep Human CD34 Positive Selection Kit II according to the manufacturer's protocol. $CD34^+$
351 HSPCs were cultured at 10^5 cells/mL in StemSpan SFEM II Medium supplemented with 100ng/mL

352 SCF, 100ng/mL TPO, 100ng/mL FLT3, 100ng/mL IL-6, 20mg/mL streptomycin, and 20U/mL
353 penicillin. Incubator conditions were 37°C, 5% CO_2, and 5% O_2.
354
355 **Genome editing of HSPCs**
356 Cas9 protein was purchased from Integrated DNA Technologies or Aldevron. Preceding
357 electroporation, ribonucleoproteins (RNPs) were complexed with guide RNAs (gRNAs) at a
358 Cas9:gRNA molar ratio of 1:2.5 at 25°C for 10-20mins. HSPCs were then resuspended in Lonza
359 P3 buffer with RNPs and subsequently electroporated using a Lonza 4D Nucleofector (program
360 DZ-100). Electroporated cells were then plated at 10^5 cells/mL in HSPC media and AAV6 was
361 added at 5×10^3 vector genomes/cell based on titers determined by droplet digital PCR (ddPCR).
362 The small molecule AZD-7648 was also added to cells to improve HDR frequencies as previously
363 reported[35].
364
365 ***In vitro* differentiation of HSPCs into erythrocytes**
366 2-3d post-targeting, HSPCs were transitioned into StemSpan SFEM II Medium supplemented
367 with 100U/mL penicillin–streptomycin, 10ng/mL SCF, 1ng/mL IL-3, 3U/mL EPO, 200µg/mL
368 transferrin, 3% antibody serum, 2% human plasma, 10µg/mL insulin, and 3U/mL heparin and
369 maintained at 10^5 cells/mL. At d7 of culture, cells were transitioned to the above media without
370 IL-3 and maintained at 10^5 cells/mL. At d11, cells were transitioned to the above media without
371 IL-3 and with transferrin increased to 1mg/mL and maintained at 10^6 cells/mL.
372
373 **Other methods**
374 Detailed explanations of HUDEP-2 cell culture, quantification of genome editing events, AAV6
375 vector preparation, high-performance liquid chromatography (HPLC), western blot, and RNA-
376 sequencing protocols are described in the Supplemental Methods section.
377
378 **Acknowledgements**
379 The authors thank the following funding sources that made this work possible: University of
380 California, San Francisco NIH T32 Research Training in Transplant Surgery Fellowship to S.N.C.;
381 American Society of Gene & Cell Therapy Career Development Award to M.K.C.; NIH NHLBI (no.
382 R01-HL161291) to M.K.C., M.H.P., and T.C.M. and funding from the UCSF Center for Maternal-
383 Fetal Precision Medicine. We thank Emma Canepa and Billie Lianoglou for their assistance with
384 patient sample collection and our patients for their gracious participation in research.
385

386 **Conflicts of interest**

387 M.H.P. is a member of the scientific advisory board of Allogene Therapeutics. M.H.P. is on the
388 Board of Directors of Graphite Bio. M.H.P. has equity in CRISPR Tx. T.C.M. is on the scientific
389 advisory board of Acrigen and receives grant funding from Novartis, BioMarin, and Biogen.
390 M.K.C., B.W., T.C.M., and M.H.P. hold patent US-20220280571-A1 and provisional patent no.
391 63/236,178.

392

393 **References**

394 1. Vichinsky E. Complexity of alpha thalassemia: growing health problem with new
395 approaches to screening, diagnosis, and therapy. *Ann N Y Acad Sci*. 2010;1202:180-
396 187.
397 2. Piel FB, Weatherall DJ. The α-Thalassemias. *New England Journal of Medicine*.
398 2014;371(20):1908-1916.
399 3. Kreger EM, Singer ST, Witt RG, et al. Favorable outcomes after in utero transfusion in
400 fetuses with alpha thalassemia major: a case series and review of the literature. *Prenat*
401 *Diagn*. 2016;36(13):1242-1249.
402 4. Schwab ME, Lianoglou BR, Gano D, et al. The impact of in utero transfusions on
403 perinatal outcomes in patients with alpha thalassemia major: the UCSF registry. *Blood*
404 *Adv*. 2023;7(2):269-279.
405 5. Schrier SL, Centis F, Verneris M, Ma L, Angelucci E. The role of oxidant injury in the
406 pathophysiology of human thalassemias. *Redox Rep*. 2003;8(5):241-245.
407 6. Baird DC, Batten SH, Sparks SK. Alpha- and Beta-thalassemia: Rapid Evidence Review.
408 *Am Fam Physician*. 2022;105(3):272-280.
409 7. Fleischhauer K, Locatelli F, Zecca M, et al. Graft rejection after unrelated donor
410 hematopoietic stem cell transplantation for thalassemia is associated with nonpermissive
411 HLA-DPB1 disparity in host-versus-graft direction. *Blood*. 2006;107(7):2984-2992.
412 8. Cromer MK, Camarena J, Martin RM, et al. Gene replacement of α-globin with β-globin
413 restores hemoglobin balance in β-thalassemia-derived hematopoietic stem and
414 progenitor cells. *Nat Med*. 2021;27(4):677-687.
415 9. Thompson AA, Walters MC, Kwiatkowski J, et al. Gene Therapy in Patients with
416 Transfusion-Dependent β-Thalassemia. *N Engl J Med*. 2018;378(16):1479-1493.
417 10. Frangoul H, Altshuler D, Cappellini MD, et al. CRISPR-Cas9 Gene Editing for Sickle Cell
418 Disease and β-Thalassemia. *New England Journal of Medicine*. 2021;384(3):252-260.

419 11. Camarena J, Luna SE, Hampton JP, et al. Using human genetics to develop strategies
420 to increase erythropoietic output from genome-edited hematopoietic stem and progenitor
421 cells. Published online August 4, 2023:2023.08.04.552064.
422 12. Chakraborty N, Bilgrami S, Maness L, et al. Myeloablative chemotherapy with
423 autologous peripheral blood stem cell transplantation for metastatic breast cancer:
424 immunologic consequences affecting clinical outcome. *Bone Marrow Transplant*.
425 1999;24(8):837-843.
426 13. Bhatia S. Long-term health impacts of hematopoietic stem cell transplantation inform
427 recommendations for follow-up. *Expert Rev Hematol*. 2011;4(4):437-452; quiz 453-454.
428 14. Inamoto Y, Shah NN, Savani BN, et al. Secondary solid cancer screening following
429 hematopoietic cell transplantation. *Bone Marrow Transplant*. 2015;50(8):1013-1023.
430 15. Selvaraj S, Feist WN, Viel S, et al. High-efficiency transgene integration by homology-
431 directed repair in human primary cells using DNA-PKcs inhibition. *Nat Biotechnol*.
432 Published online August 3, 2023:1-14.
433 16. Dever DP, Bak RO, Reinisch A, et al. CRISPR/Cas9 β-globin gene targeting in human
434 haematopoietic stem cells. *Nature*. 2016;539(7629):384-389.
435 17. Kurita R, Suda N, Sudo K, et al. Establishment of Immortalized Human Erythroid
436 Progenitor Cell Lines Able to Produce Enucleated Red Blood Cells. *PLOS ONE*.
437 2013;8(3):e59890.
438 18. Conant D, Hsiau T, Rossi N, et al. Inference of CRISPR Edits from Sanger Trace Data.
439 *CRISPR J*. 2022;5(1):123-130.
440 19. Brinkman EK, Chen T, Amendola M, van Steensel B. Easy quantitative assessment of
441 genome editing by sequence trace decomposition. *Nucleic Acids Res*.
442 2014;42(22):e168.
443 20. Cradick TJ, Qiu P, Lee CM, Fine EJ, Bao G. COSMID: A Web-based Tool for Identifying
444 and Validating CRISPR/Cas Off-target Sites. *Mol Ther Nucleic Acids*. 2014;3(12):e214.
445 21. Cromer MK, Majeti KR, Rettig GR, et al. Comparative analysis of CRISPR off-target
446 discovery tools following ex vivo editing of CD34+ hematopoietic stem and progenitor
447 cells. *Mol Ther*. 2023;31(4):1074-1087.
448 22. Vakulskas CA, Dever DP, Rettig GR, et al. A high-fidelity Cas9 mutant delivered as a
449 ribonucleoprotein complex enables efficient gene editing in human hematopoietic stem
450 and progenitor cells. *Nat Med*. 2018;24(8):1216-1224.

451 23. Dulmovits BM, Appiah-Kubi AO, Papoin J, et al. Pomalidomide reverses γ-globin
452 silencing through the transcriptional reprogramming of adult hematopoietic progenitors.
453 *Blood*. 2016;127(11):1481-1492.
454 24. de la Chapelle A, Träskelin AL, Juvonen E. Truncated erythropoietin receptor causes
455 dominantly inherited benign human erythrocytosis. *Proc Natl Acad Sci U S A*.
456 1993;90(10):4495-4499.
457 25. Vichinsky EP. Clinical Manifestations of α-Thalassemia. *Cold Spring Harb Perspect Med*.
458 2013;3(5):a011742.
459 26. Scott MD. H2O2 injury in beta thalassemic erythrocytes: protective role of catalase and
460 the prooxidant effects of GSH. *Free Radic Biol Med*. 2006;40(7):1264-1272.
461 27. Gregory GL, Wienert B, Schwab M, et al. Investigating Zeta Globin Gene Expression to
462 Develop a Potential Therapy for Alpha Thalassemia Major. *Blood*. 2020;136:3-4.
463 28. Hendel A, Bak RO, Clark JT, et al. Chemically modified guide RNAs enhance CRISPR-
464 Cas genome editing in human primary cells. *Nat Biotechnol*. 2015;33(9):985-989.
465 29. Khan IF, Hirata RK, Russell DW. AAV-mediated gene targeting methods for human
466 cells. *Nat Protoc*. 2011;6(4):482-501.
467 30. Aurnhammer C, Haase M, Muether N, et al. Universal real-time PCR for the detection
468 and quantification of adeno-associated virus serotype 2-derived inverted terminal repeat
469 sequences. *Hum Gene Ther Methods*. 2012;23(1):18-28.
470 31. Eden E, Navon R, Steinfeld I, Lipson D, Yakhini Z. GOrilla: a tool for discovery and
471 visualization of enriched GO terms in ranked gene lists. *BMC Bioinformatics*.
472 2009;10(1):48.
473 32. Allen F, Crepaldi L, Alsinet C, et al. Predicting the mutations generated by repair of
474 Cas9-induced double-strand breaks. *Nat Biotechnol*. 2019;37(1):64-72.
475
476
477
478
479

Figure 1

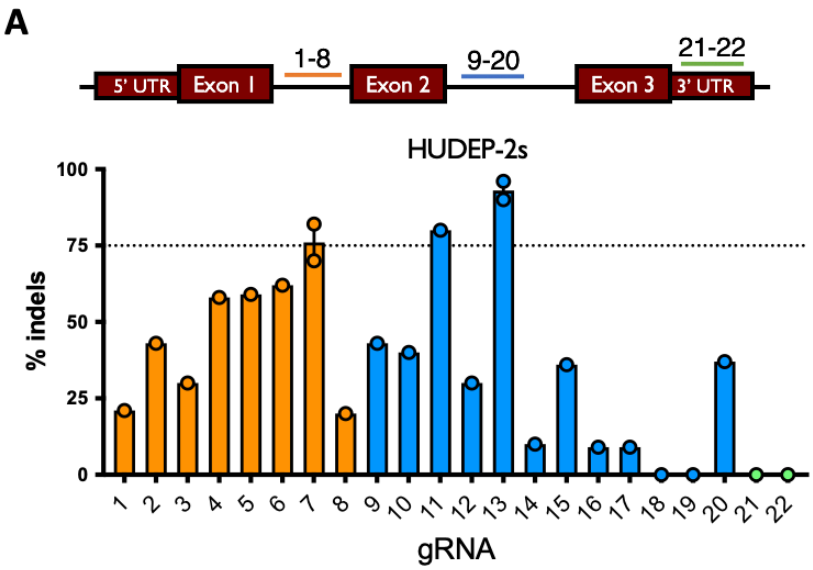

B

Guide	Distance from nearest exon	# COSMID OTs ≤5.5
sg7	21bp	19
sg11	60bp	77
sg13	79bp	56

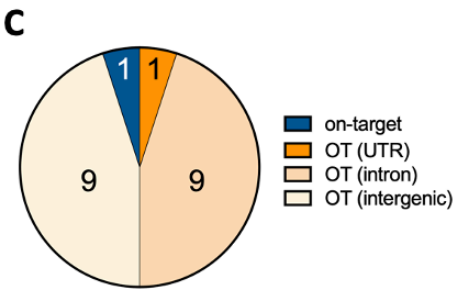

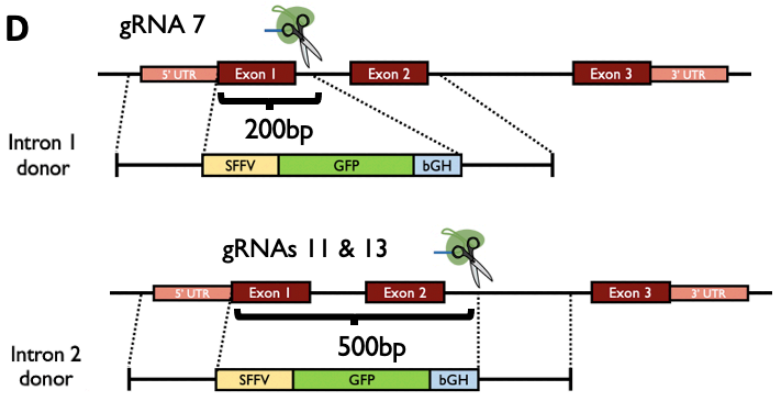

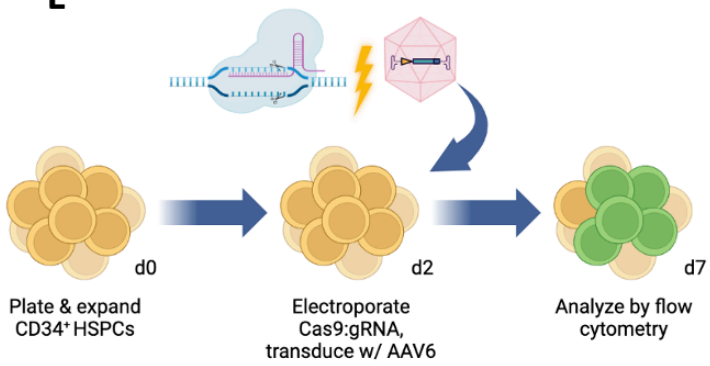

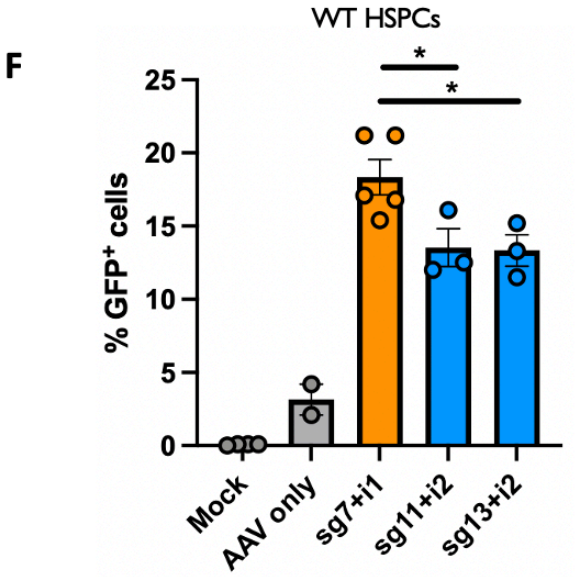

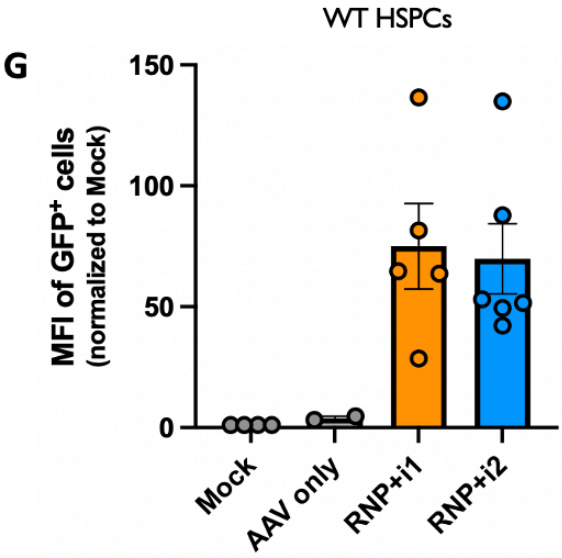

481 **Figure 1. Efficient integration of HDR templates at *HBB* locus.**
482 (A) Schematic of *HBB*-targeting gRNAs and resulting indel frequencies in HUDEP-2 cells
483 following electroporation-mediated delivery of Cas9:gRNA RNPs. Dotted line indicates indel
484 frequencies at 75% threshold. Bars represent mean ± standard error of the mean (SEM). (B) *In*
485 *silico* off-target analysis of gRNA 7, 11, 13 using COSMID. (C) Pie chart displaying genomic
486 features at 19 predicted target sites for sg7. (D) Schematic of custom AAV6 DNA repair donors
487 designed to mediate integration at intron 1 using sg7 or intron 2 using sg11 or 13. Bracket
488 indicates distance between left and right homology arms. (E) Schematic of Cas9/AAV6 genome
489 editing workflow in primary HSPCs. (F) Percentage of GFP^+ cells following editing in WT HSPCs
490 was determined at d5 post-editing using flow cytometry. Bars represent mean ± SEM. * denotes
491 $p<0.05$ by unpaired two-tailed t-test. (G) Mean fluorescence intensity (MFI) of GFP^+ cells from
492 Figure 1F was determined by flow cytometry. Bars represent mean ± SEM.
493

Figure 2

A

UTRs	Gene
HBB	*HBA1*
HBA1	*HBA1*
HBA2	*HBA2*

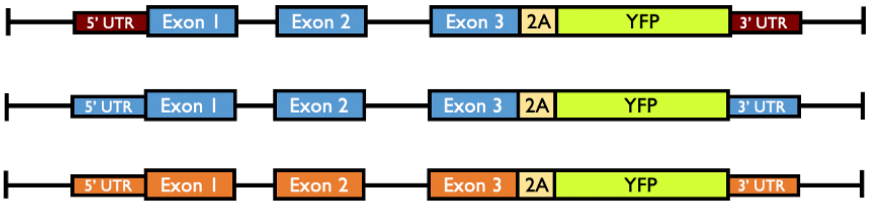

B

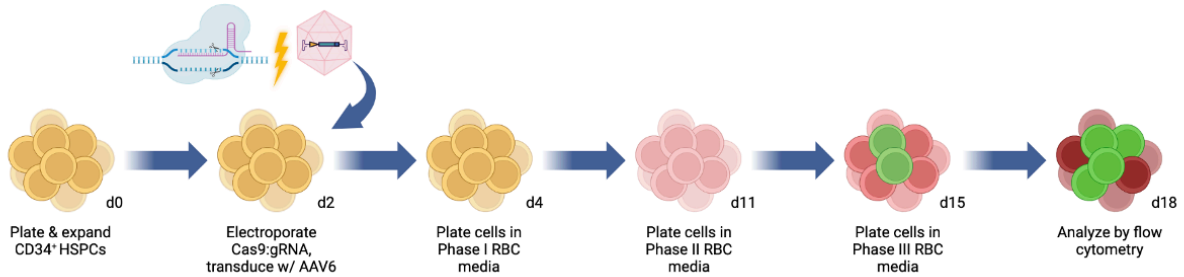

C

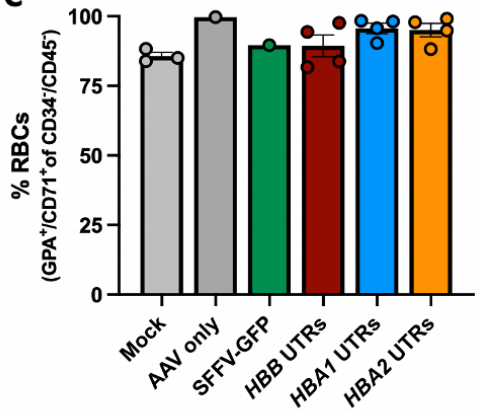

D

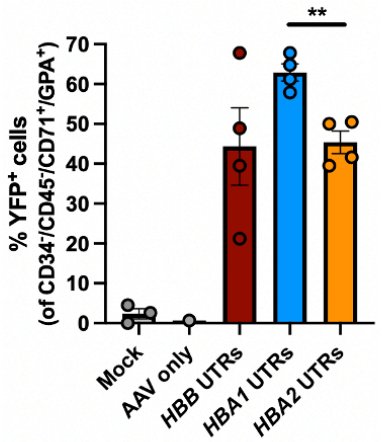

E

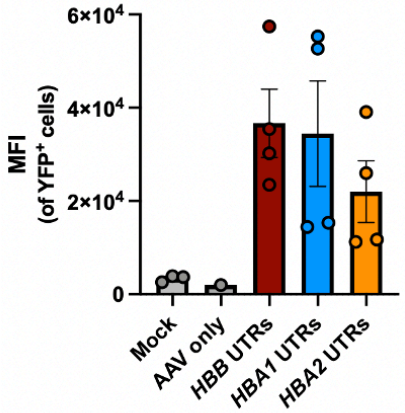

F

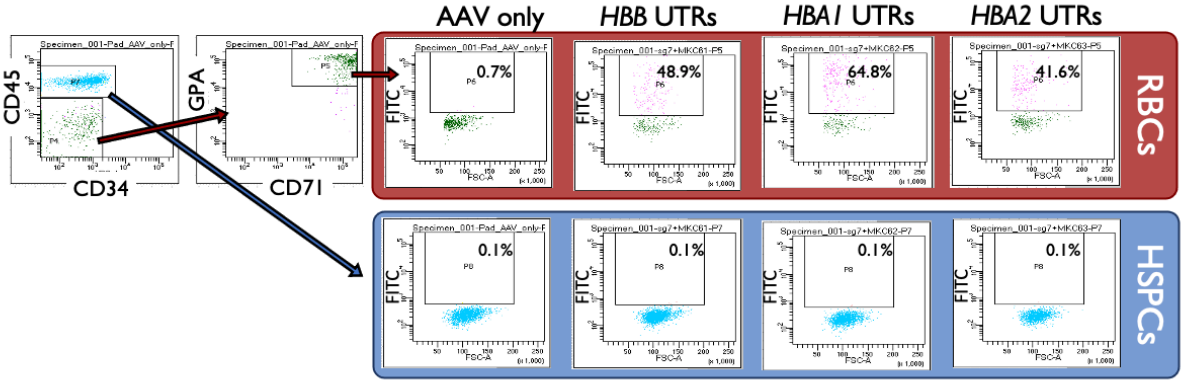

G

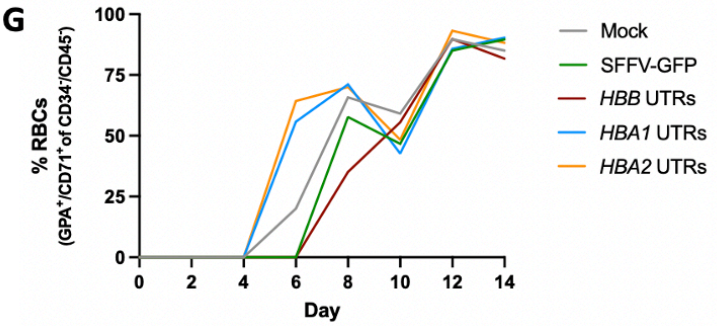

H

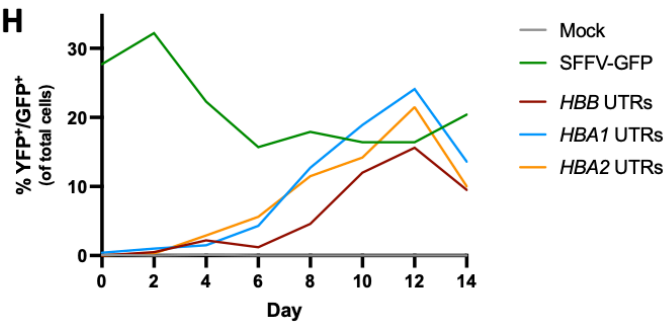

495 **Figure 2. Integration at *HBB* drives erythroid-specific expression of transgenes.**
496 (A) Schematic of custom AAV6 DNA repair donors designed to integrate promoterless *HBA-2A-*
497 *YFP* transgenes at the start codon of *HBB*. Table to the left indicates whether cassette integrated
498 *HBA1* or *HBA2* transgene as well as *HBB*, *HBA1*, or *HBA2* UTRs. (B) Schematic of Cas9/AAV6
499 genome editing workflow in primary HSPCs followed by *in vitro* RBC differentiation. (C)
500 Percentage of $CD34^{-}/CD45^{-}$ HSPCs acquiring RBC surface markers—GPA and CD71—as
501 determined by flow cytometry. Bars represent mean ± SEM. (D) Percentage of YFP^{+} cells in
502 $CD34^{-}/CD45^{-}/CD71^{+}/GPA^{+}$ cells was determined at d14 of RBC differentiation using flow
503 cytometry. Bars represent mean ± SEM. ** denotes $p<0.005$. (E) MFI of YFP^{+} cells from Figure
504 2D was determined by flow cytometry. Bars represent mean ± SEM. (F) At d11 of RBC
505 differentiation, cells were stained for HSPC/RBC markers and analyzed by flow cytometry.
506 Percentage of YFP^{+} cells are noted (N=1) (G) Percentage of $CD34^{-}/CD45^{-}$ cells that acquired
507 CD71 and GPA RBC markers are plotted over the course of RBC differentiation (N=1). (H)
508 Percentage of YFP^{+} or GFP^{+} cells are plotted over the course of RBC differentiation (N=1).
509

Figure 3

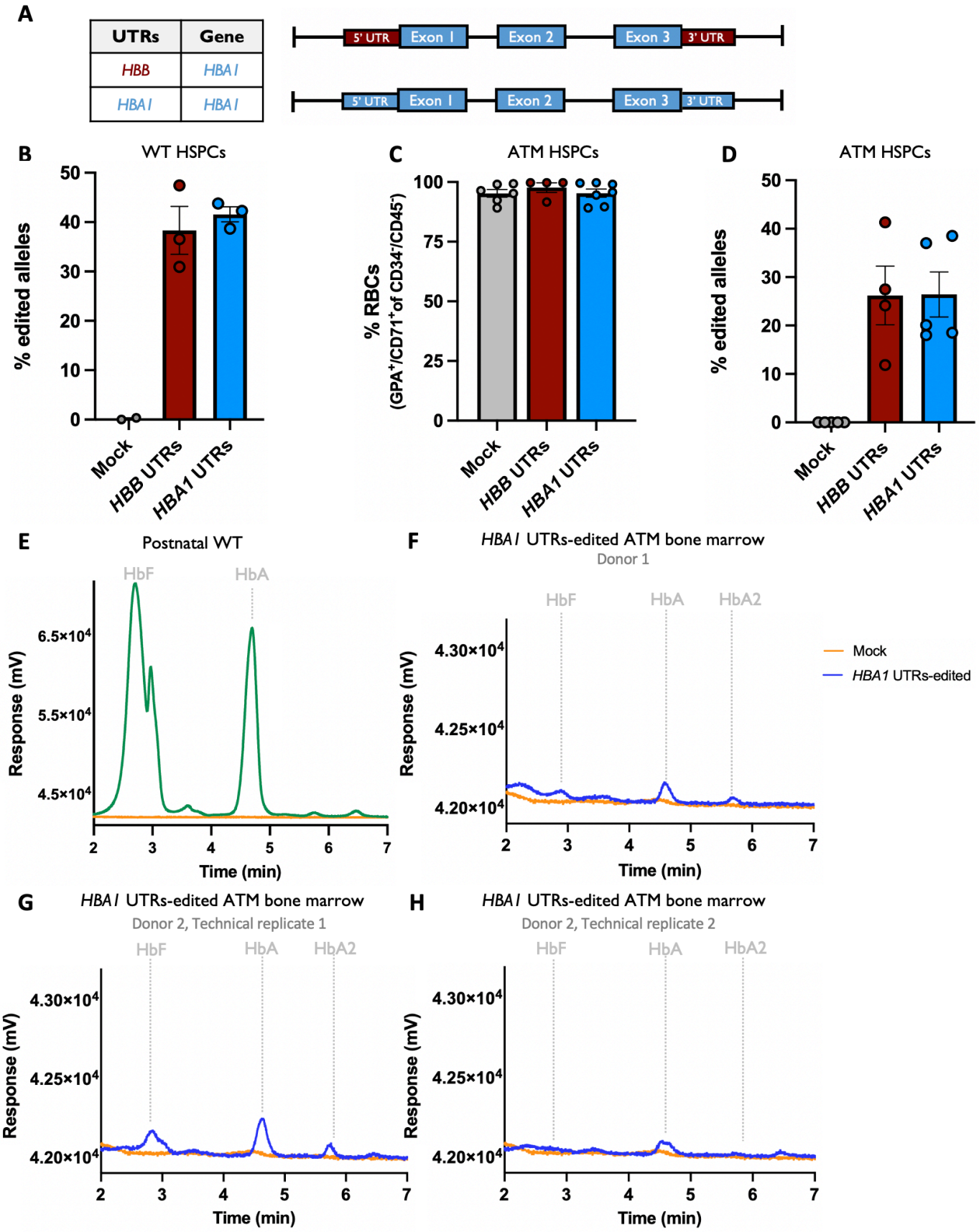
A
UTRs
Gene
HBB
HBA1
HBA1
HBA1
5' UTR
Exon 1
Exon 2
Exon 3
3' UTR
B
WT HSPCs
% edited alleles
Mock
HBB UTRs
HBA1 UTRs
C
ATM HSPCs
% RBCs
(GPA+/CD71+of CD34-/CD45-)
D
ATM HSPCs
% edited alleles
E
Postnatal WT
HbF
HbA
Response (mV)
Time (min)
F
HBA1 UTRs-edited ATM bone marrow
Donor 1
HbA2
Mock
HBA1 UTRs-edited
G
HBA1 UTRs-edited ATM bone marrow
Donor 2, Technical replicate 1
H
HBA1 UTRs-edited ATM bone marrow
Donor 2, Technical replicate 2

511 **Figure 3. α-globin integration yields low levels of hemoglobin in αTM HSPCs**
512 (A) Schematic of custom AAV6 DNA repair donors designed to integrate promoterless *HBA*
513 transgenes at the start codon of *HBB*. Table to the left indicates whether the cassette integrated
514 *HBA1* transgene with *HBB* or *HBA1* UTRs. (B) Percentage of edited alleles in WT HSPCs at d14
515 of RBC differentiation. Bars represent mean ± SEM. (C) Percentage of $CD34^-/CD45^-$ αTM
516 HSPCs acquiring RBC surface markers—GPA and CD71—as determined by flow cytometry. Bars
517 represent mean ± SEM. (D) Percentage of edited alleles in αTM HSPCs at d14 of RBC
518 differentiation. Bars represent mean ± SEM. (E) HPLC elution chromatogram displaying the
519 hemoglobin tetramer profile from WT healthy control HSPCs following *in vitro* RBC differentiation.
520 Time displayed on the x-axis represents retention time in minutes for each hemoglobin tetramer
521 type to elute. Absorbance on the y-axis indicates the concentration of a particular hemoglobin
522 tetramer. (F-H) HPLC elution chromatograms displaying the hemoglobin tetramer profile from
523 αTM HSPCs that have undergone editing and RBC differentiation. Chromatograms represent 2
524 different donors as well as a technical replicate from donor 2 that was edited independently.
525

Figure 4

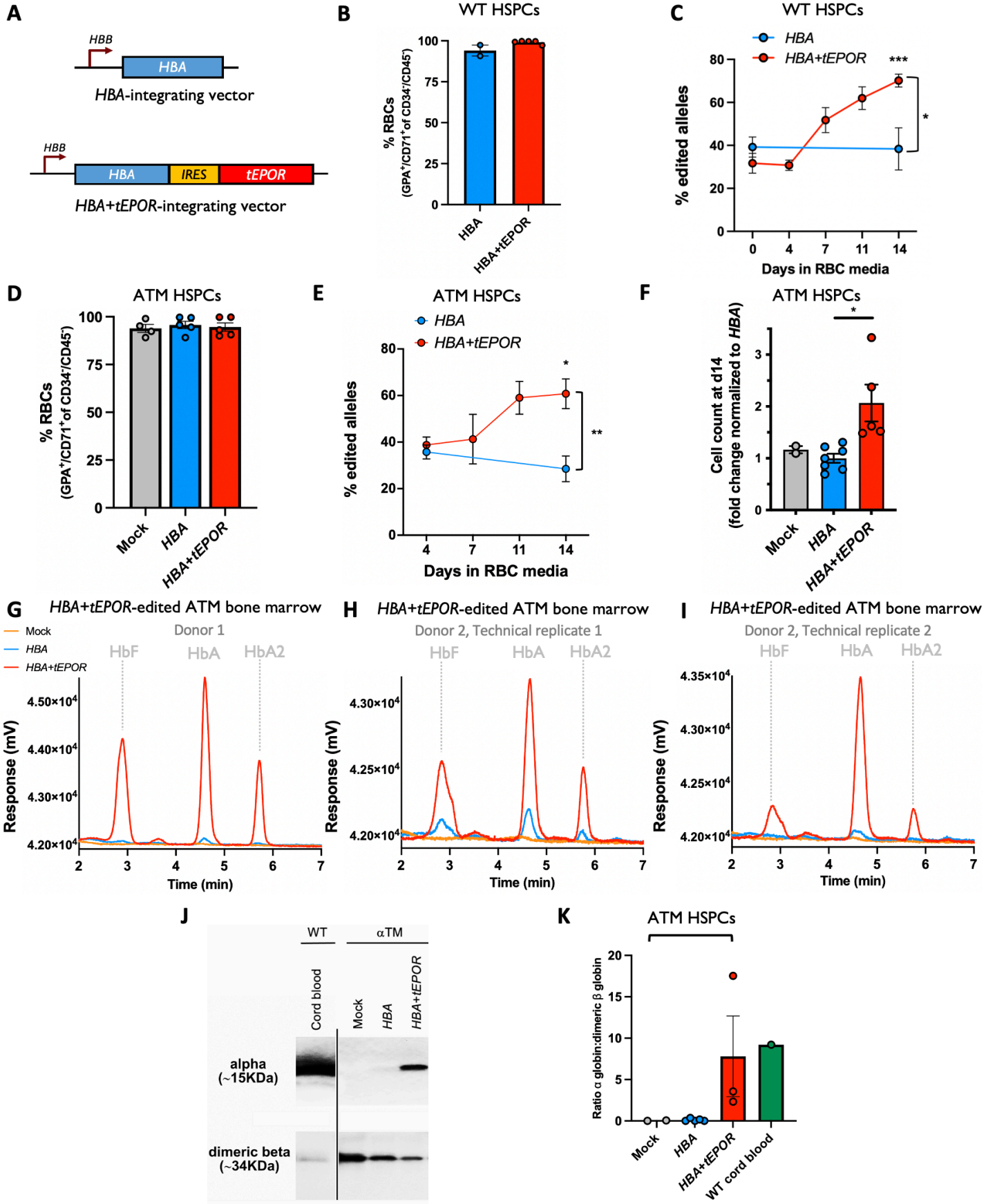
A
HBB
HBA
HBA-integrating vector
HBB
HBA
IRES
tEPOR
HBA+tEPOR-integrating vector
B
WT HSPCs
% RBCs (GPA+/CD71+ of CD34-/CD45-)
HBA
HBA+tEPOR
C
WT HSPCs
HBA
HBA+tEPOR
% edited alleles
Days in RBC media
D
ATM HSPCs
% RBCs (GPA+/CD71+ of CD34-/CD45-)
Mock
HBA
HBA+tEPOR
E
ATM HSPCs
HBA
HBA+tEPOR
% edited alleles
Days in RBC media
F
ATM HSPCs
Cell count at d14 (fold change normalized to HBA)
Mock
HBA
HBA+tEPOR
G
HBA+tEPOR-edited ATM bone marrow
Donor 1
Mock
HBA
HBA+tEPOR
HbF
HbA
HbA2
Response (mV)
Time (min)
H
HBA+tEPOR-edited ATM bone marrow
Donor 2, Technical replicate 1
HbF
HbA
HbA2
Response (mV)
Time (min)
I
HBA+tEPOR-edited ATM bone marrow
Donor 2, Technical replicate 2
HbF
HbA
HbA2
Response (mV)
Time (min)
J
WT
αTM
Cord blood
Mock
HBA
HBA+tEPOR
alpha (~15KDa)
dimeric beta (~34KDa)
K
ATM HSPCs
Ratio α globin:dimeric β globin
Mock
HBA
HBA+tEPOR
WT cord blood

527 **Figure 4. Dual integration of α-globin and *tEPOR* increases hemoglobin production in αTM**
528 **HSPCs**
529 (A) Schematic of custom AAV6 donors designed to integrate promoterless *HBA* and *HBA+tEPOR*
530 transgenes at start codon of HBB. Both vectors are flanked by *HBA1* UTRs. (B) Percentage of
531 $CD34^-/CD45^-$ WT HSPCs acquiring RBC surface markers—GPA and CD71—as determined by
532 flow cytometry. Bars represent mean ± SEM. (C) Percentage of edited alleles in WT HSPCs over
533 the course of RBC differentiation. Bars represent mean ± SEM. *** denotes p=0.0004 and *
534 denotes p=0.01. (D) Percentage of $CD34^-/CD45^-$ αTM HSPCs acquiring GPA and CD71 as
535 determined by flow cytometry. Bars represent mean ± SEM. (E) Percentage of edited alleles in
536 αTM HSPCs over the course of RBC differentiation. Bars represent mean ± SEM. ** denotes
537 p=0.009 and * denotes p=0.02. (F) Cell count at d14 of RBC differentiation with fold change
538 normalized to *HBA*. Bars represent mean ± SEM. ** denotes p=0.007. (G-I) Hemoglobin tetramer
539 HPLC elution chromatograms. Chromatograms represent 2 different donors as well as a technical
540 replicate from donor 2 that was edited independently. (J) Western blot of mock and edited αTM
541 HSPCs at the end of RBC differentiation compared to WT umbilical cord blood-derived RBCs.
542 Western blot image was taken from a single gel that was cropped to place wild-type control next
543 to treated conditions, as indicated by the black line. Loading was standardized by using the same
544 number of cells for input. (K) Ratio of α-globin to dimeric β-globin quantification from western blot.
545 Bars represent mean ± SEM.
546

Figure 5

A

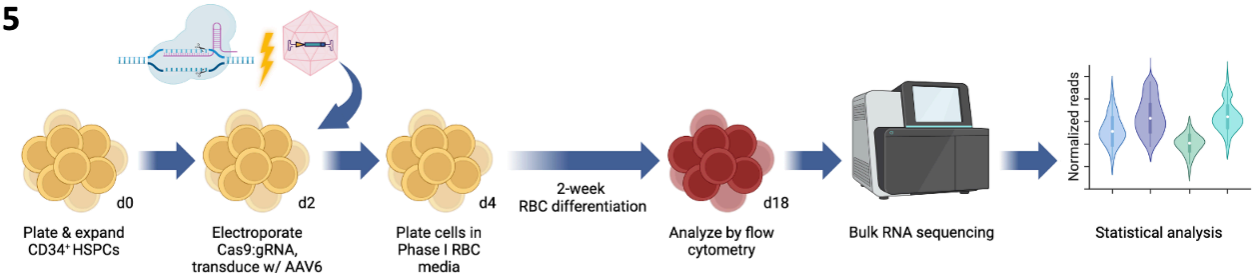

B

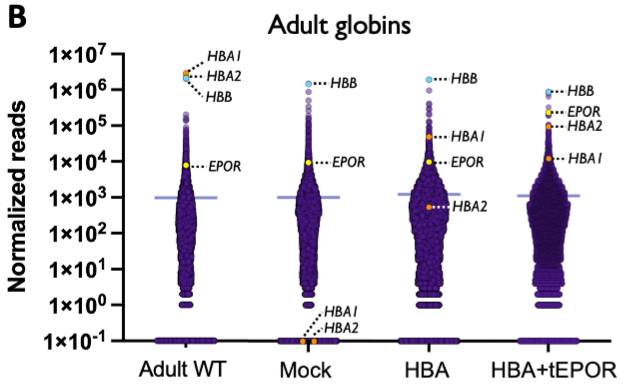

C

Rank	WT Mock	HBA Mock	HBA+tEPOR Mock
1	*HBA1*	*HBA1*	*HBA2*
2	*HBA2*	*GPI*	*SCD*
3	*HBM*	*LPIN2*	*HBA1*
4	*TRIB3*	*BNIP3*	*EPOR*
5	*H1F0*	*RPL9*	*INSIG1*

D

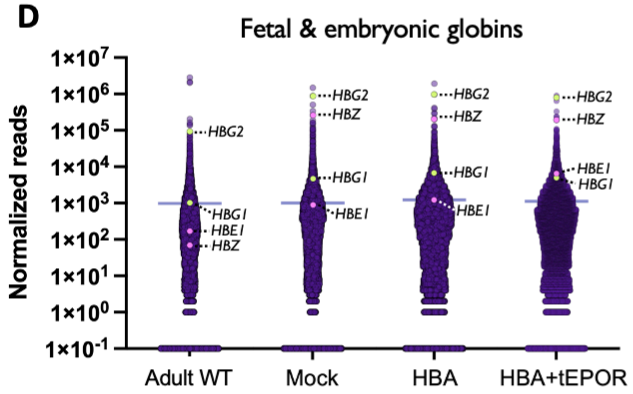

E

Rank	Mock WT	HBA WT	HBA+tEPOR WT
1	*HBZ*	*HBZ*	*HBZ*
2	*HSPA1A*	*HSPA1A*	*SCD*
3	*NME4*	*HPD*	*HSPA1A*
4	*HSPA1B*	*SYNPO2L*	*EPOR*
5	*SYNPO2L*	*NME4*	*INSIG1*

F

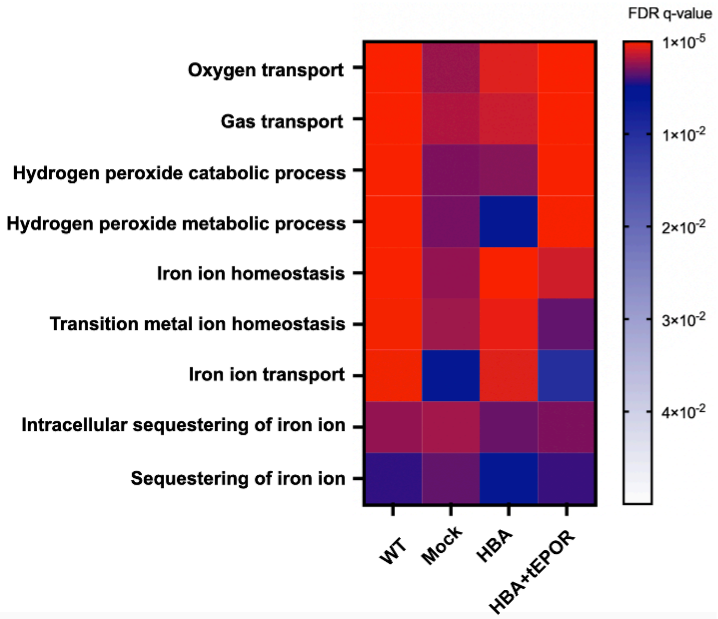

G

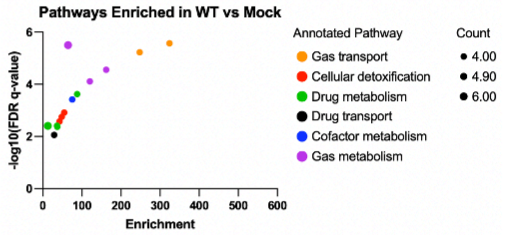

H

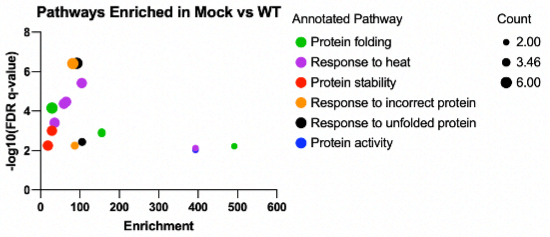

I

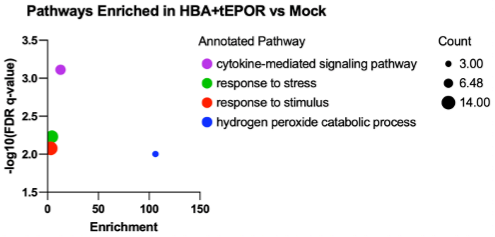

548 **Figure 5. Bulk RNA-sequencing of edited αTM HSPCs demonstrates restoration of α-globin**
549 **gene expression and oxygen transport and iron ion metabolic processes**
550 (A) Schematic of bulk RNA-sequencing workflow. (B) Normalized reads across all samples
551 displayed with specific genes *HBA1*, *HBA2*, *HBB*, and *EPOR* highlighted. A count of "0.1" was
552 assigned to *HBA1* and *HBA2* for display purposes. (C) Table displaying top 5 genes with the
553 greatest rank change comparing WT and edited αTM cells to mock. (D) Normalized reads across
554 all samples displayed with fetal and embryonic globin genes *HBG1*, *HBG2*, *HBE1*, and *HBZ*
555 highlighted. (E) Table displaying top 5 genes with the greatest rank change comparing mock and
556 edited αTM cells to WT. (F) Heatmap of FDR q-values across 9 commonly enriched GO
557 processes across conditions. Input for GO analysis was the top 0.001% most highly expressed
558 genes within each condition. (G-I) Bubble plots depicting enriched GO processes across
559 treatment comparisons; y-axis displays significance by $-\log_{10}$(FDR q-value) and x-axis displays
560 enrichment. Color of bubble pertains to GO process and size of bubble pertains to number of
561 genes represented in the respective GO process. Input for GO analysis was the top 0.001% of
562 genes showing greatest rank change for each comparison (shown in label above each panel).

Figure 1

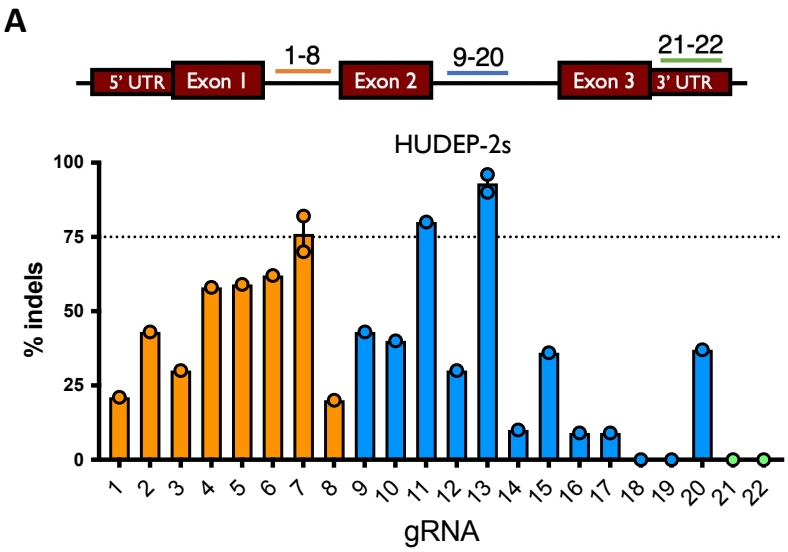

B

Guide	Distance from nearest exon	# COSMID OTs ≤5.5
sg7	21bp	19
sg11	60bp	77
sg13	79bp	56

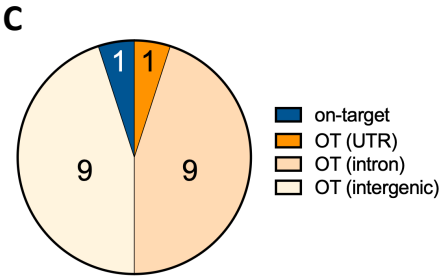

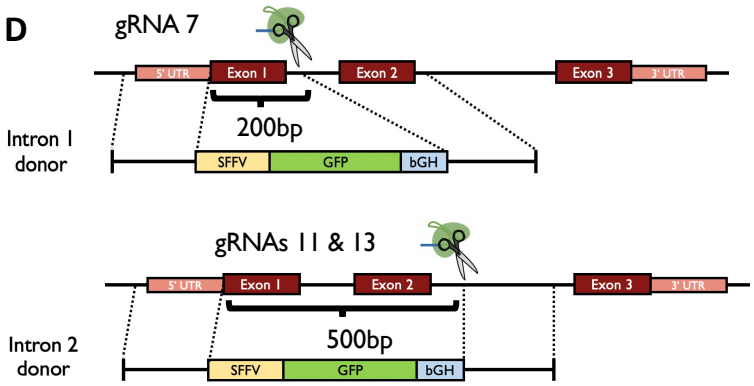

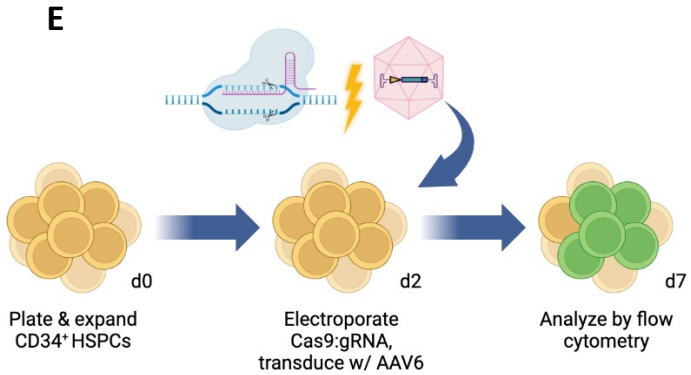

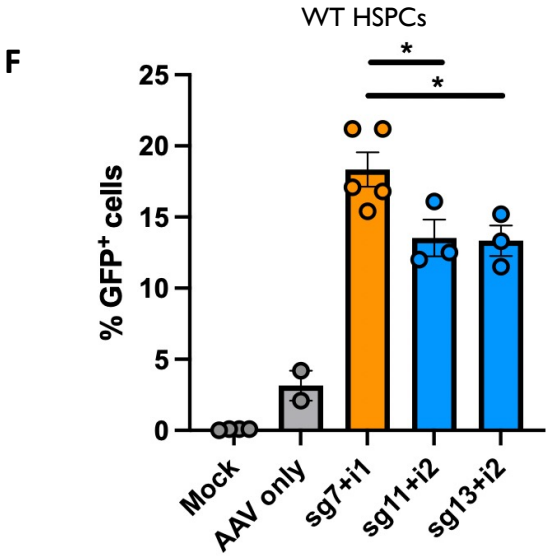

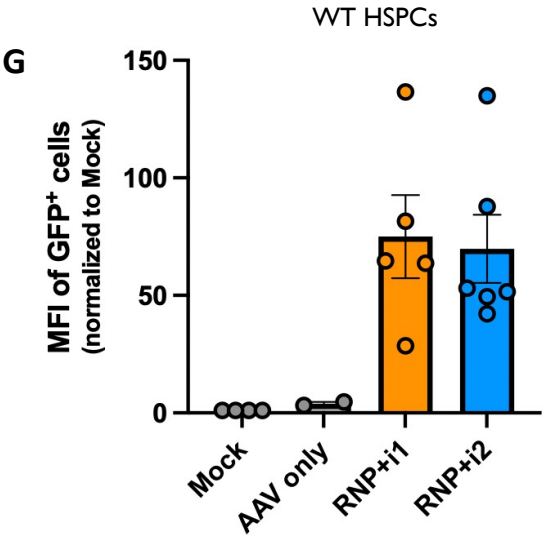

Figure 2

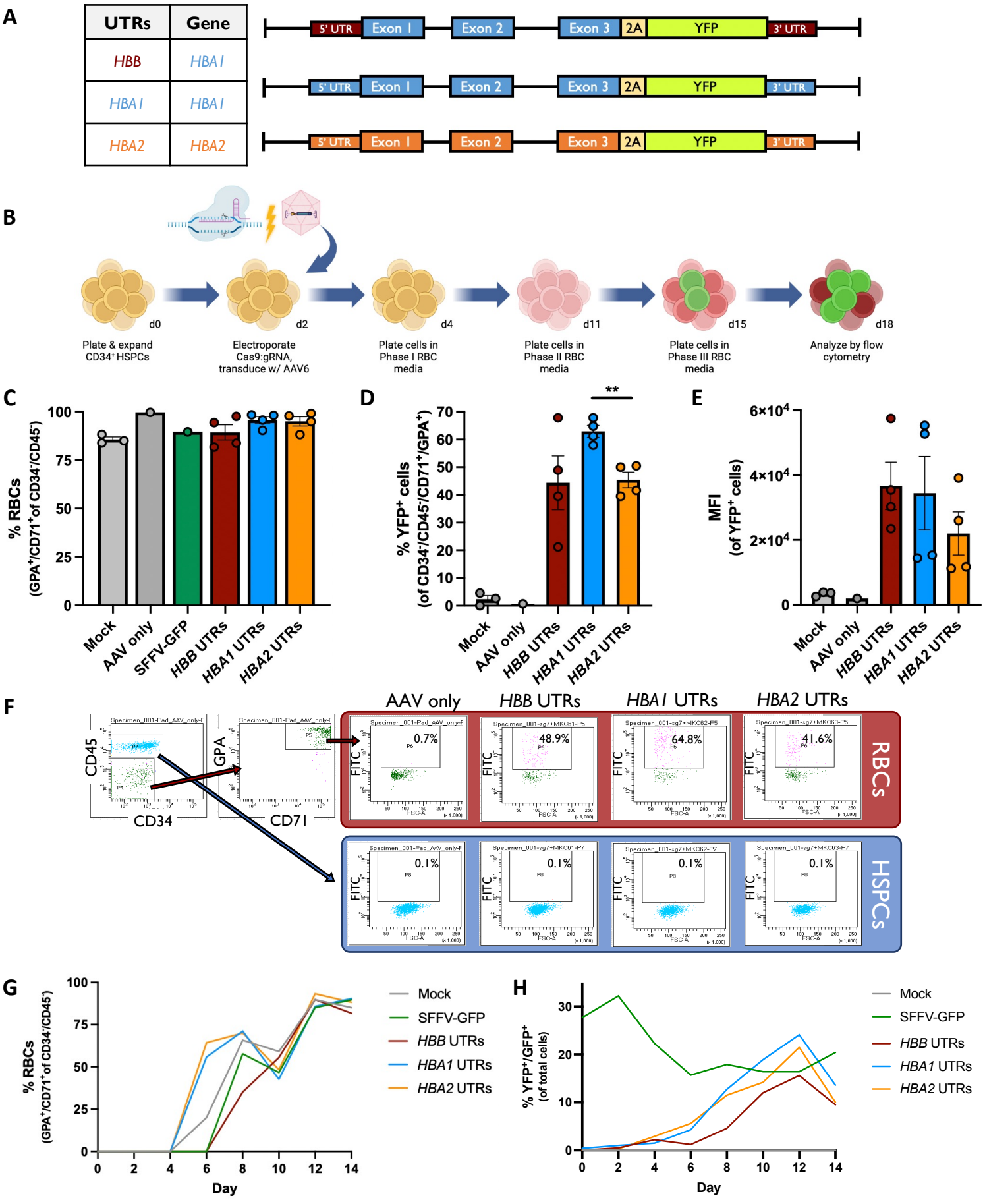
A
UTRs
Gene
HBB
HBA1
HBA1
HBA1
HBA2
HBA2
5' UTR
Exon 1
Exon 2
Exon 3
2A
YFP
3' UTR
B
d0
d2
d4
d11
d15
d18
Plate & expand CD34+ HSPCs
Electroporate Cas9:gRNA, transduce w/ AAV6
Plate cells in Phase I RBC media
Plate cells in Phase II RBC media
Plate cells in Phase III RBC media
Analyze by flow cytometry
C
% RBCs (GPA+/CD71+ of CD34-/CD45-)
Mock
AAV only
SFFV-GFP
HBB UTRs
HBA1 UTRs
HBA2 UTRs
D
% YFP+ cells (of CD34-/CD45-/CD71+/GPA+)
**
E
MFI (of YFP+ cells)
F
CD45
CD34
GPA
CD71
AAV only
HBB UTRs
HBA1 UTRs
HBA2 UTRs
0.7%
48.9%
64.8%
41.6%
0.1%
0.1%
0.1%
0.1%
RBCs
HSPCs
G
% RBCs (GPA+/CD71+ of CD34-/CD45-)
Day
Mock
SFFV-GFP
HBB UTRs
HBA1 UTRs
HBA2 UTRs
H
% YFP+/GFP+ (of total cells)
Day

Figure 3

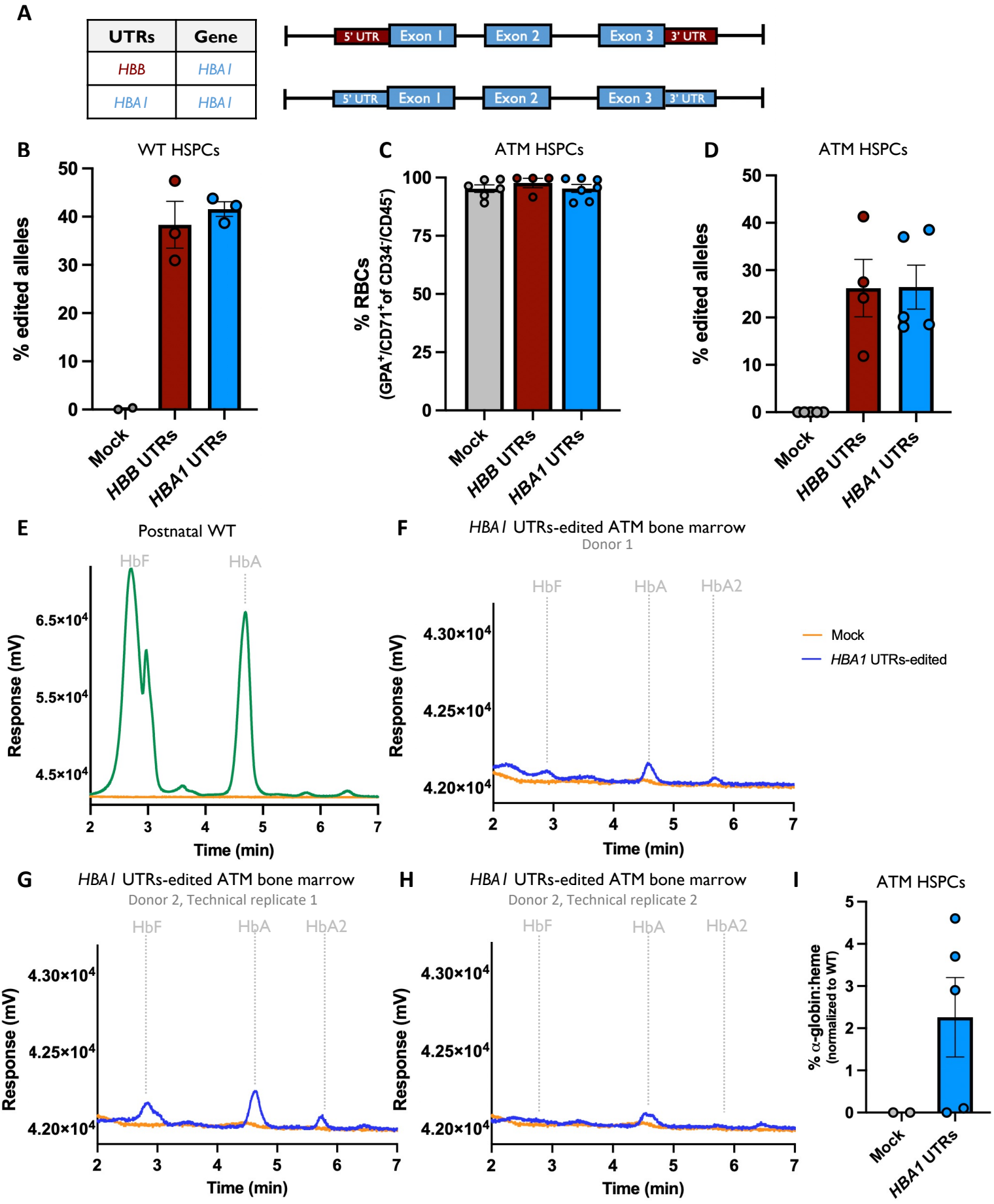
A
UTRs
Gene
HBB
HBA1
HBA1
HBA1
5' UTR
Exon 1
Exon 2
Exon 3
3' UTR
B
WT HSPCs
% edited alleles
Mock
HBB UTRs
HBA1 UTRs
C
ATM HSPCs
% RBCs
(GPA+/CD71+of CD34-/CD45-)
D
ATM HSPCs
% edited alleles
E
Postnatal WT
HbF
HbA
Response (mV)
Time (min)
F
HBA1 UTRs-edited ATM bone marrow
Donor 1
HbA2
Mock
HBA1 UTRs-edited
G
HBA1 UTRs-edited ATM bone marrow
Donor 2, Technical replicate 1
H
HBA1 UTRs-edited ATM bone marrow
Donor 2, Technical replicate 2
I
ATM HSPCs
% α-globin:heme
(normalized to WT)

Figure 4

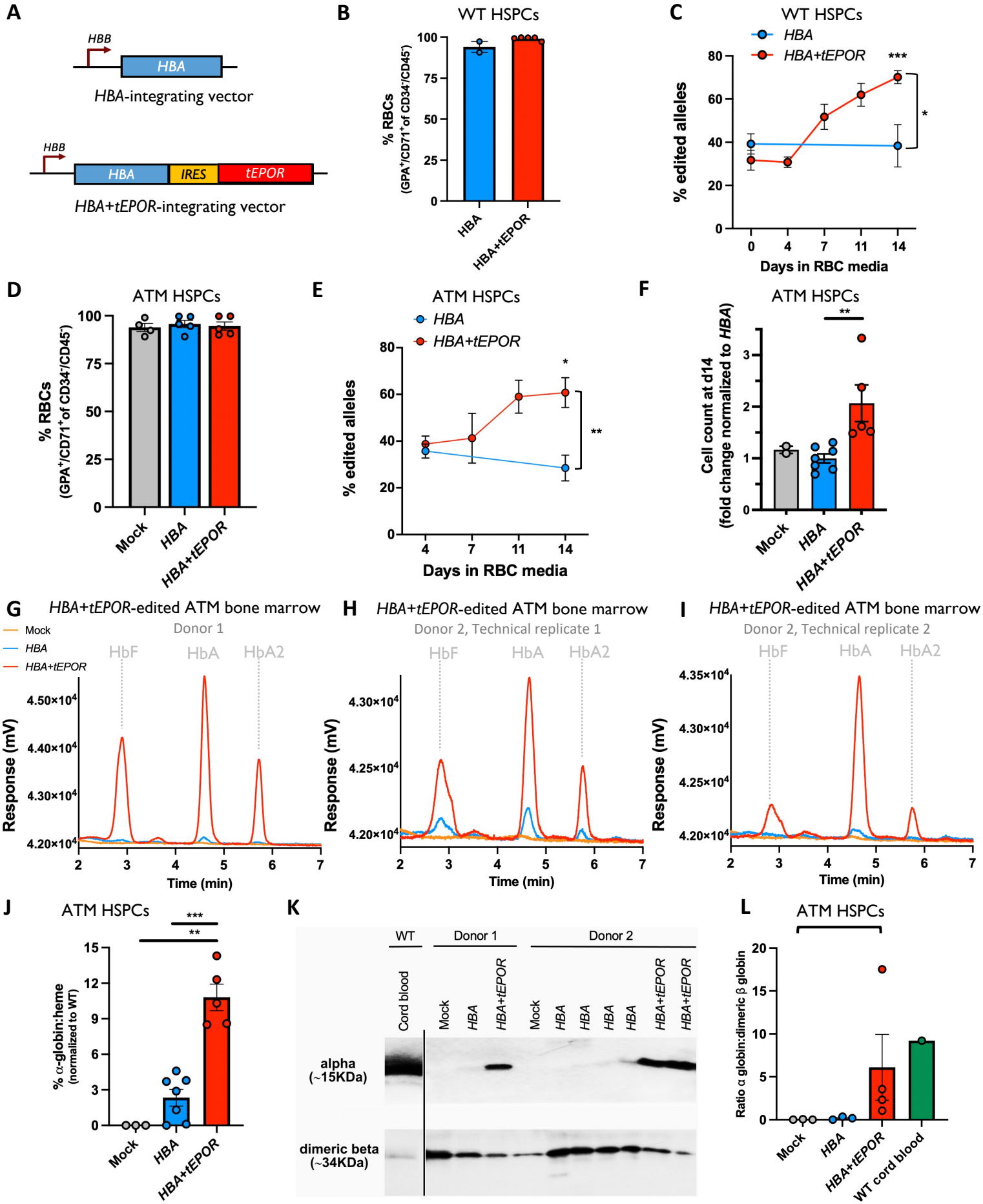
A
HBB
HBA
HBA-integrating vector
HBB
HBA
IRES
tEPOR
HBA+tEPOR-integrating vector
B
WT HSPCs
% RBCs
(GPA+/CD71+of CD34-/CD45-)
HBA
HBA+tEPOR
C
WT HSPCs
HBA
HBA+tEPOR
% edited alleles
Days in RBC media
D
ATM HSPCs
% RBCs
(GPA+/CD71+of CD34-/CD45-)
Mock
HBA
HBA+tEPOR
E
ATM HSPCs
HBA
HBA+tEPOR
% edited alleles
Days in RBC media
F
ATM HSPCs
Cell count at d14
(fold change normalized to HBA)
Mock
HBA
HBA+tEPOR
G
HBA+tEPOR-edited ATM bone marrow
Donor 1
Mock
HBA
HBA+tEPOR
HbF
HbA
HbA2
Response (mV)
Time (min)
H
HBA+tEPOR-edited ATM bone marrow
Donor 2, Technical replicate 1
HbF
HbA
HbA2
Response (mV)
Time (min)
I
HBA+tEPOR-edited ATM bone marrow
Donor 2, Technical replicate 2
HbF
HbA
HbA2
Response (mV)
Time (min)
J
ATM HSPCs
% α-globin:heme
(normalized to WT)
Mock
HBA
HBA+tEPOR
K
WT
Donor 1
Donor 2
Cord blood
Mock
HBA
HBA+tEPOR
Mock
HBA
HBA
HBA
HBA
HBA+tEPOR
HBA+tEPOR
alpha
(~15KDa)
dimeric beta
(~34KDa)
L
ATM HSPCs
Ratio α globin:dimeric β globin
Mock
HBA
HBA+tEPOR
WT cord blood

Figure 5

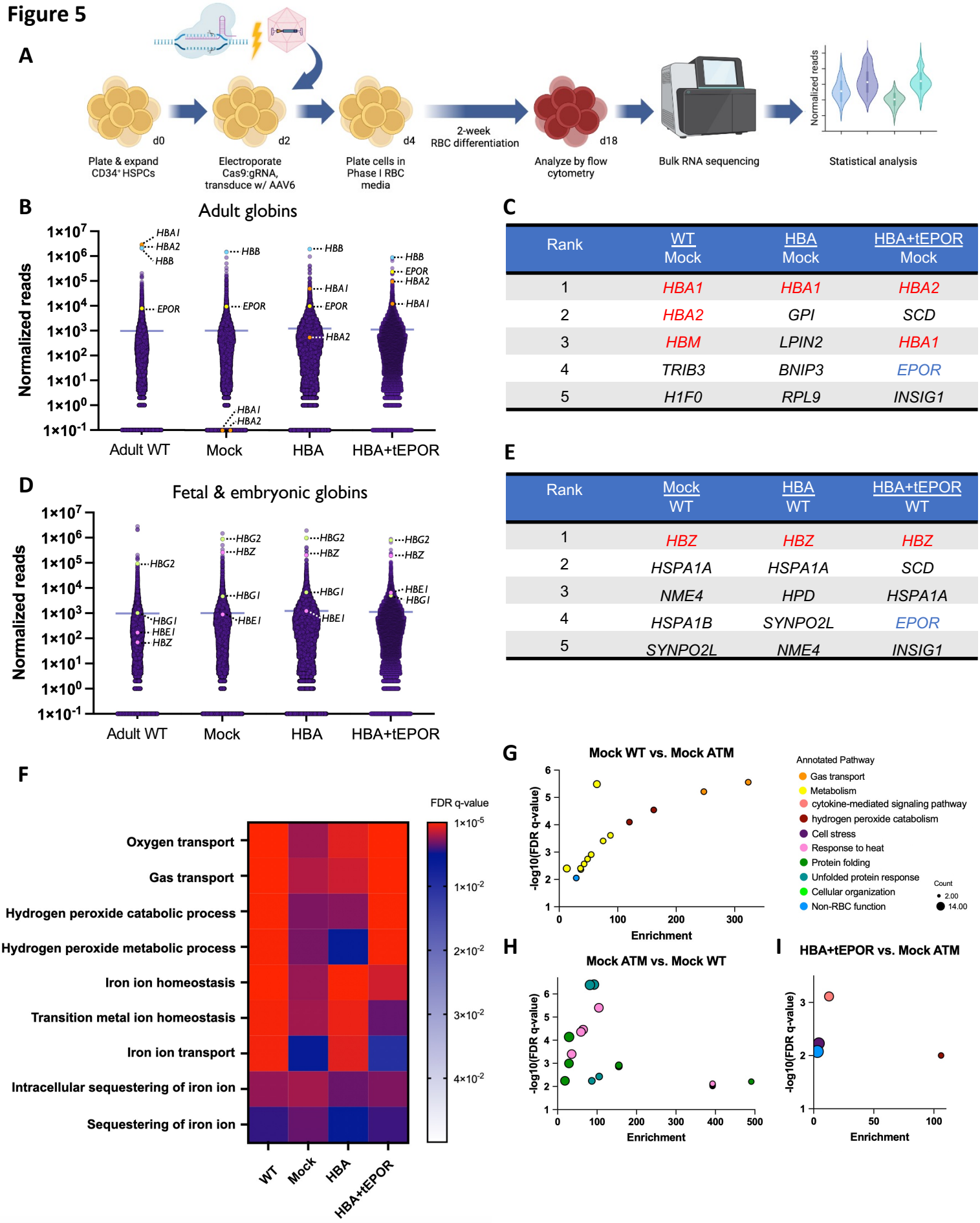

Rank	WT Mock	HBA Mock	HBA+tEPOR Mock
1	*HBA1*	*HBA1*	*HBA2*
2	*HBA2*	*GPI*	*SCD*
3	*HBM*	*LPIN2*	*HBA1*
4	*TRIB3*	*BNIP3*	*EPOR*
5	*H1F0*	*RPL9*	*INSIG1*

Rank	Mock WT	HBA WT	HBA+tEPOR WT
1	*HBZ*	*HBZ*	*HBZ*
2	*HSPA1A*	*HSPA1A*	*SCD*
3	*NME4*	*HPD*	*HSPA1A*
4	*HSPA1B*	*SYNPO2L*	*EPOR*
5	*SYNPO2L*	*NME4*	*INSIG1*

Supplemental Table 1

Guide	Location	Sequence (PAM)	% indels	Primary indel	FORECasT prediction	Nearest exon
1	intron 1	TGGTATCAAGGTTACAAGAC(AGG)	21	-5	+1	Exon 1; 19bp
2	intron 1	AAGGTTACAAGACAGGTTTA(AGG)	43	+1	+1	Exon 1; 26bp
3	intron 1	TCCACATGCCCAGTTTCTAT(TGG)	30	-10	-8	Exon 1; 41bp
4	intron 1	TAAGGAGACCAATAGAAACT(GGG)	58	+1	-1	Exon 1; 44bp
5	intron 1	ACCAATAGAAACTGGGCATG(TGG)	59	-7	+1	Exon 1; 51bp
6	intron 1	TGGAGACAGAGAAGACTCTT(GGG)	62	-2	-2	Exon 2; 59bp
7	intron 1	GGGTGGGAAAATAGACCAAT(AGG)	76	-8	-8	Exon 2; 21bp
8	intron 1	CACTGACTCTCTCTGCCTAT(TGG)	20	-3	+1	Exon 2; 25bp
9	intron 2	ACTTAACCATAGAAAAGAAG(GGG)	43	-3	-3	Exon 2; 37bp
10	intron 2	TTCTTTCCCCTTCTTTTCTA(TGG)	40	+1	-5	Exon 2; 42bp
11	intron 2	TATGGTTAAGTTCATGTCAT(AGG)	80	-5	-5	Exon 2; 60bp
12	intron 2	TTAAGTTCATGTCATAGGAA(GGG)	30	-4	-1	Exon 2; 65bp
13	intron 2	TAGGAAGGGGATAAGTAACA(GGG)	93	+1	-1	Exon 2; 79bp
14	intron 2	AACAGGGTACAGTTTAGAAT(GGG)	10	-17	-2	Exon 2; 95bp
15	intron 2	GACGAATGATTGCATCAGTG(TGG)	36	+1	+1	Exon 2; 123bp
16	intron 2	TGCATCAGTGTGGAAGTCTC(AGG)	9	+1	+1	Exon 2; 133bp
17	intron 2	AAGTATAATAGTAAAAATTG(CGG)	9	+1	+1	Exon 2; 224bp
18	intron 2	TTTTGTTATACACAATGTTA(AGG)	0	-	-	Exon 2; 251bp
19	intron 2	TTAACATTGTGTATAACAAA(AGG)	0	-	-	Exon 2; 264bp
20	intron 2	ATTCCAAATAGTAATGTACT(AGG)	37	+1	+1	Exon 2; 328bp
21	3’ UTR	AAGGAACCTTTAATAGAAAT(TGG)	0	-	-	Exon 3; 23bp
22	3’ UTR	TGCTGTCCAATTTCTATTAA(AGG)	0	-	-	Exon 3; 28bp

Supplemental Figure 1

A sg7 indel spectrum

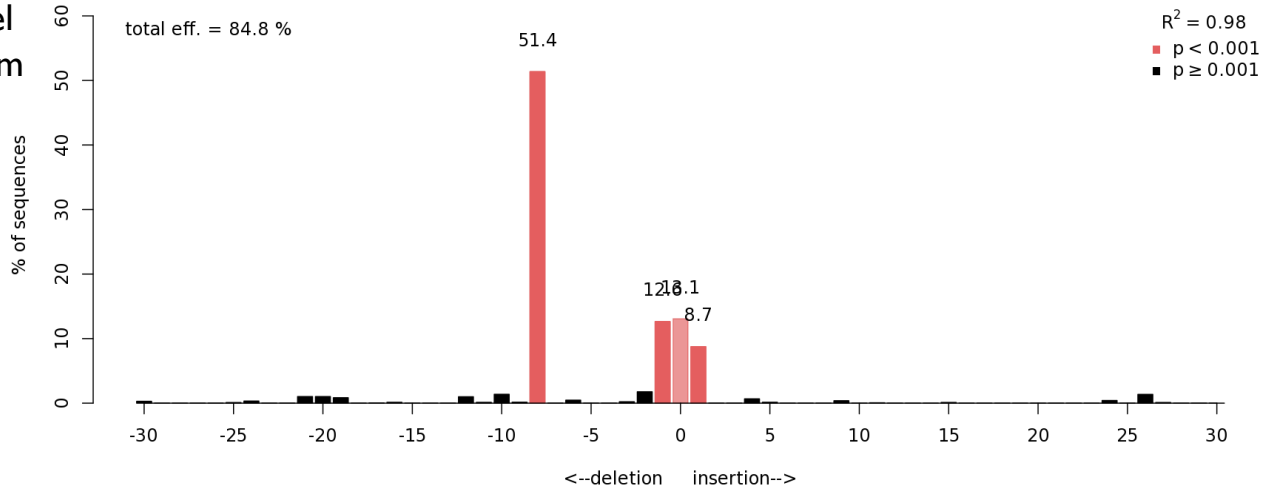

B

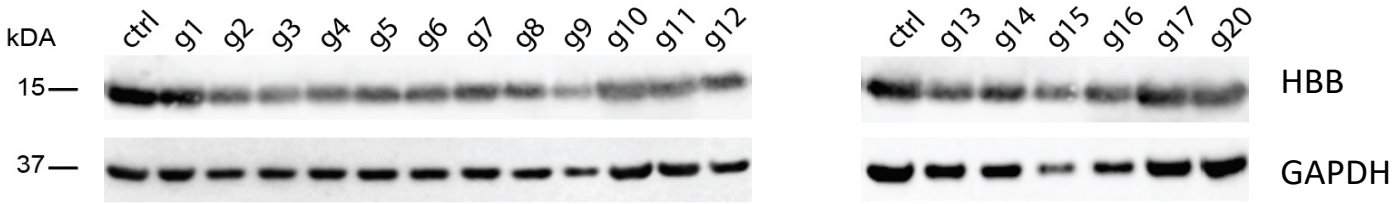

Supplemental Figure 2

A

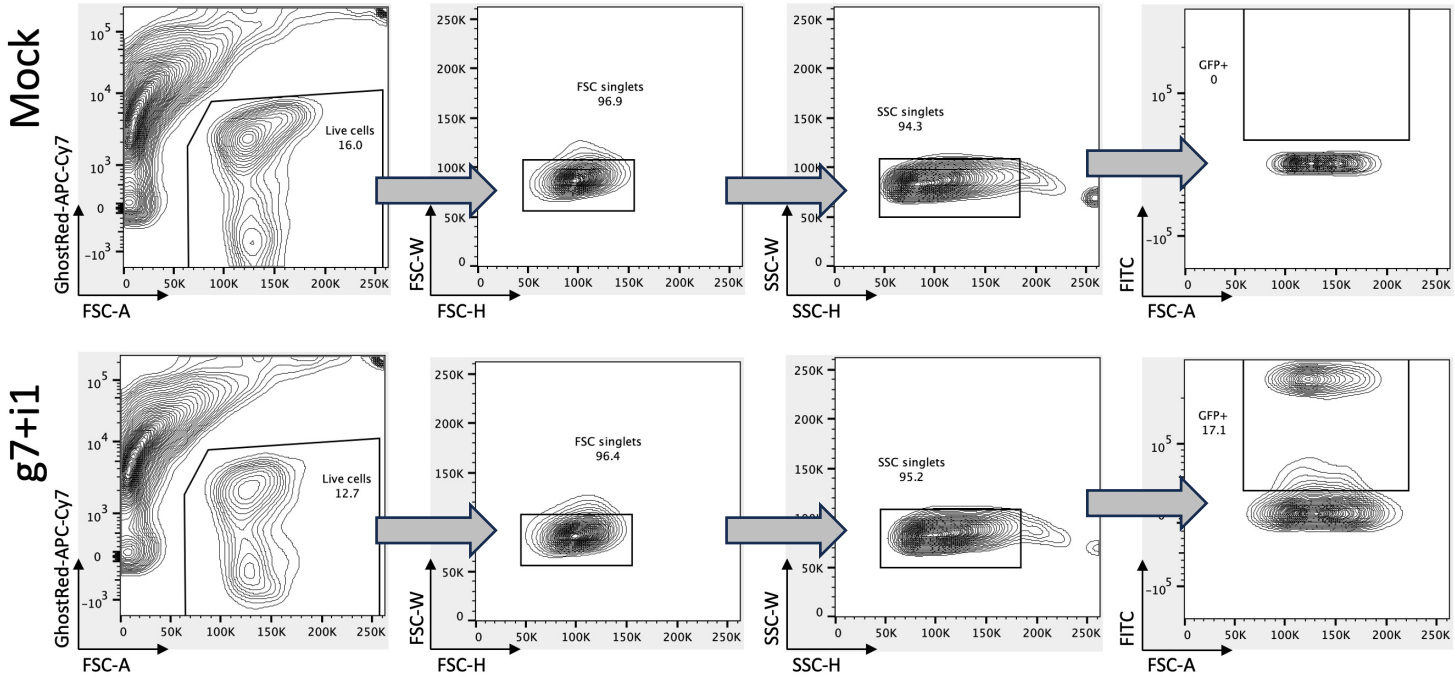

B

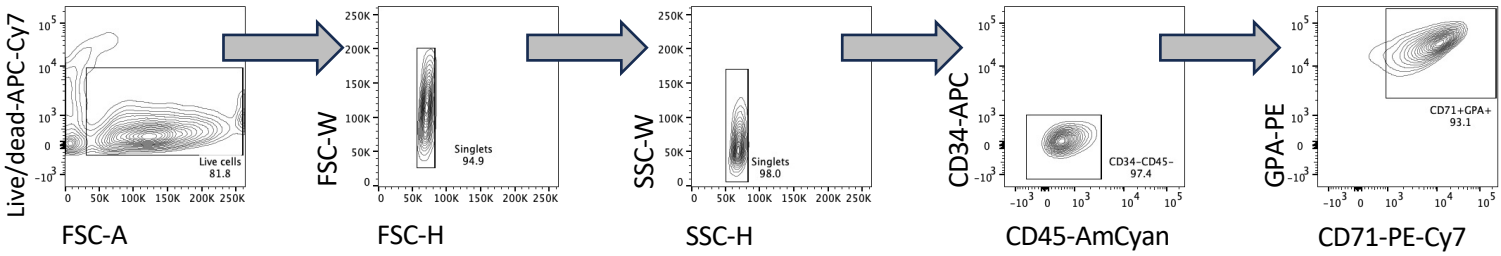

Supplemental Figure 3

A

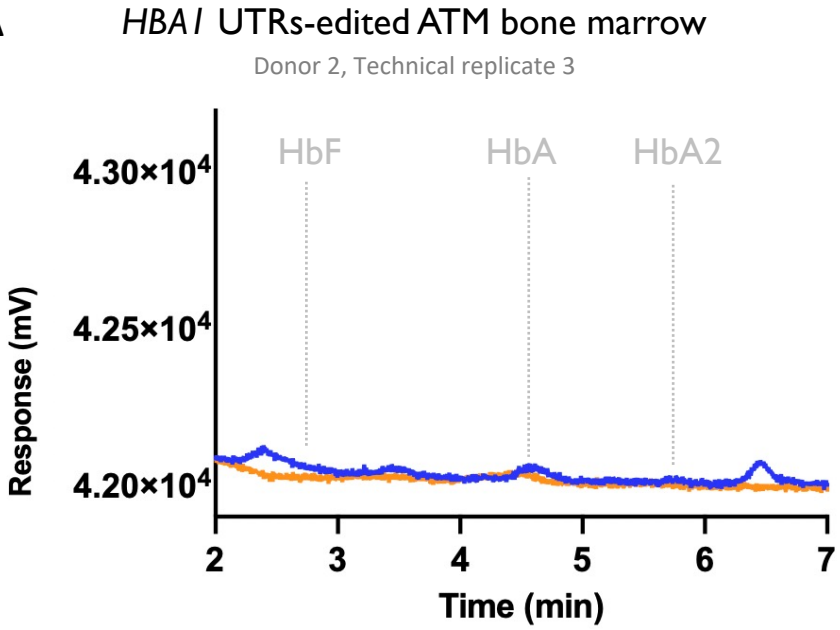

B

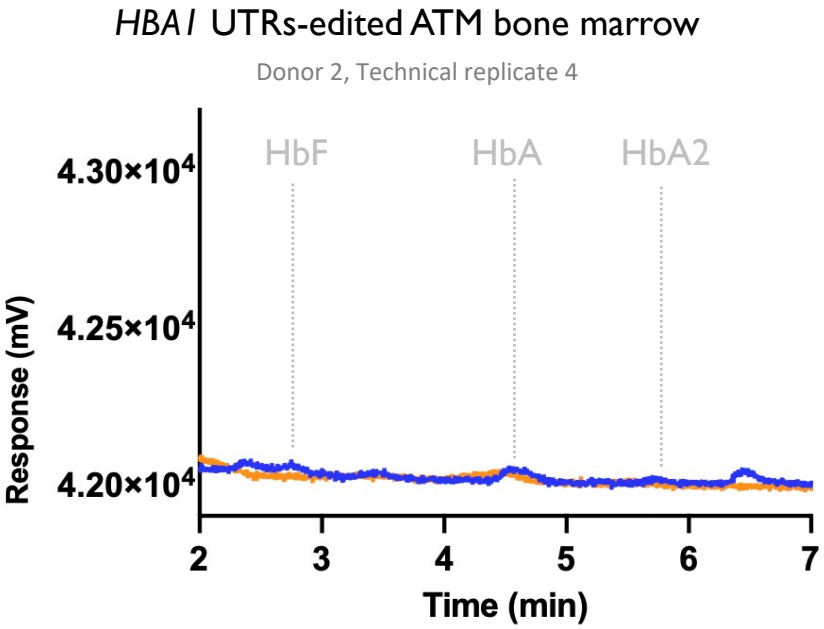

Supplemental Figure 4

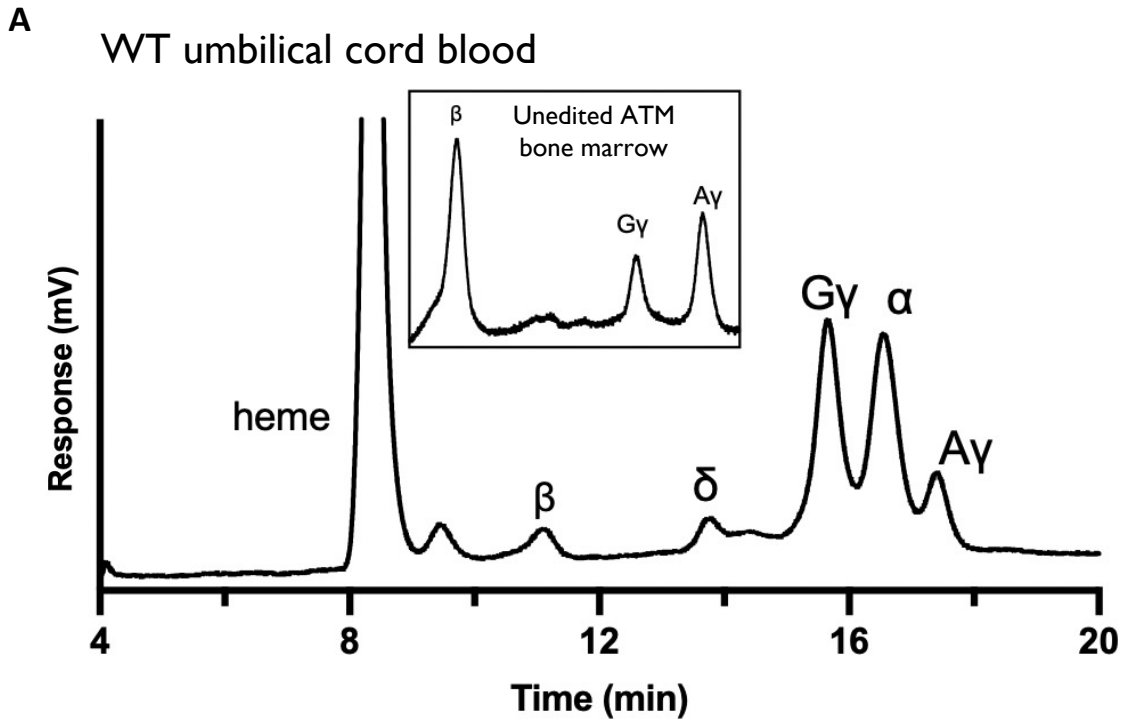

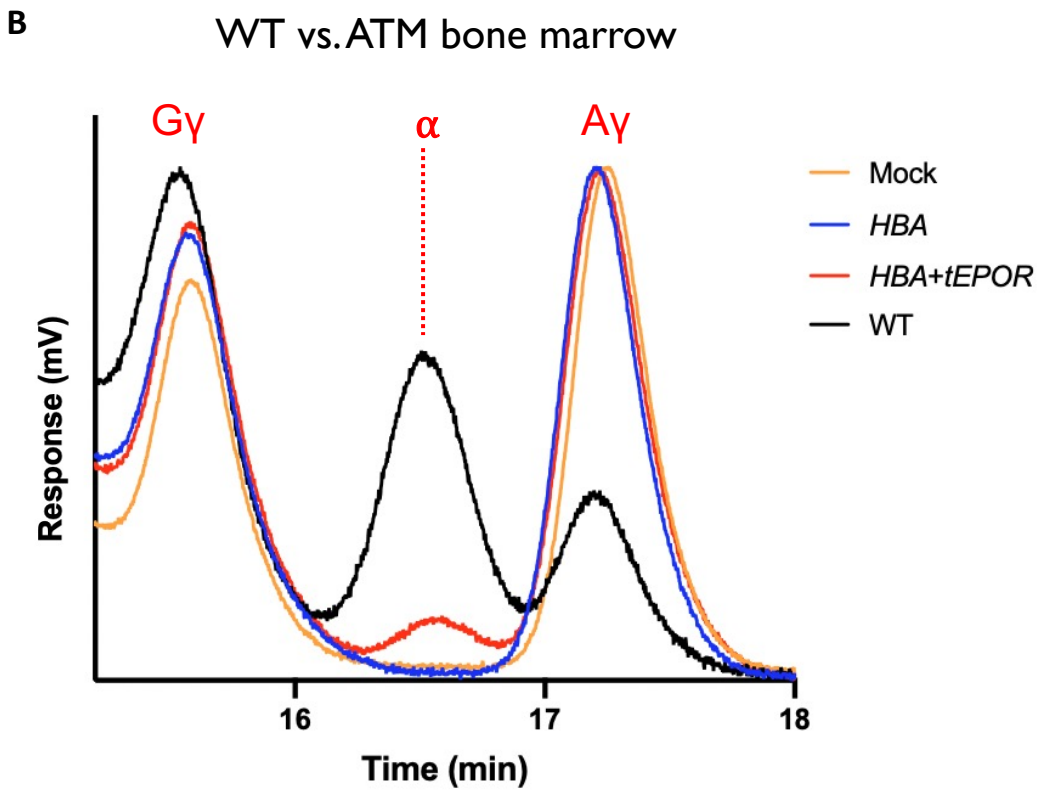

Supplemental Figure 5

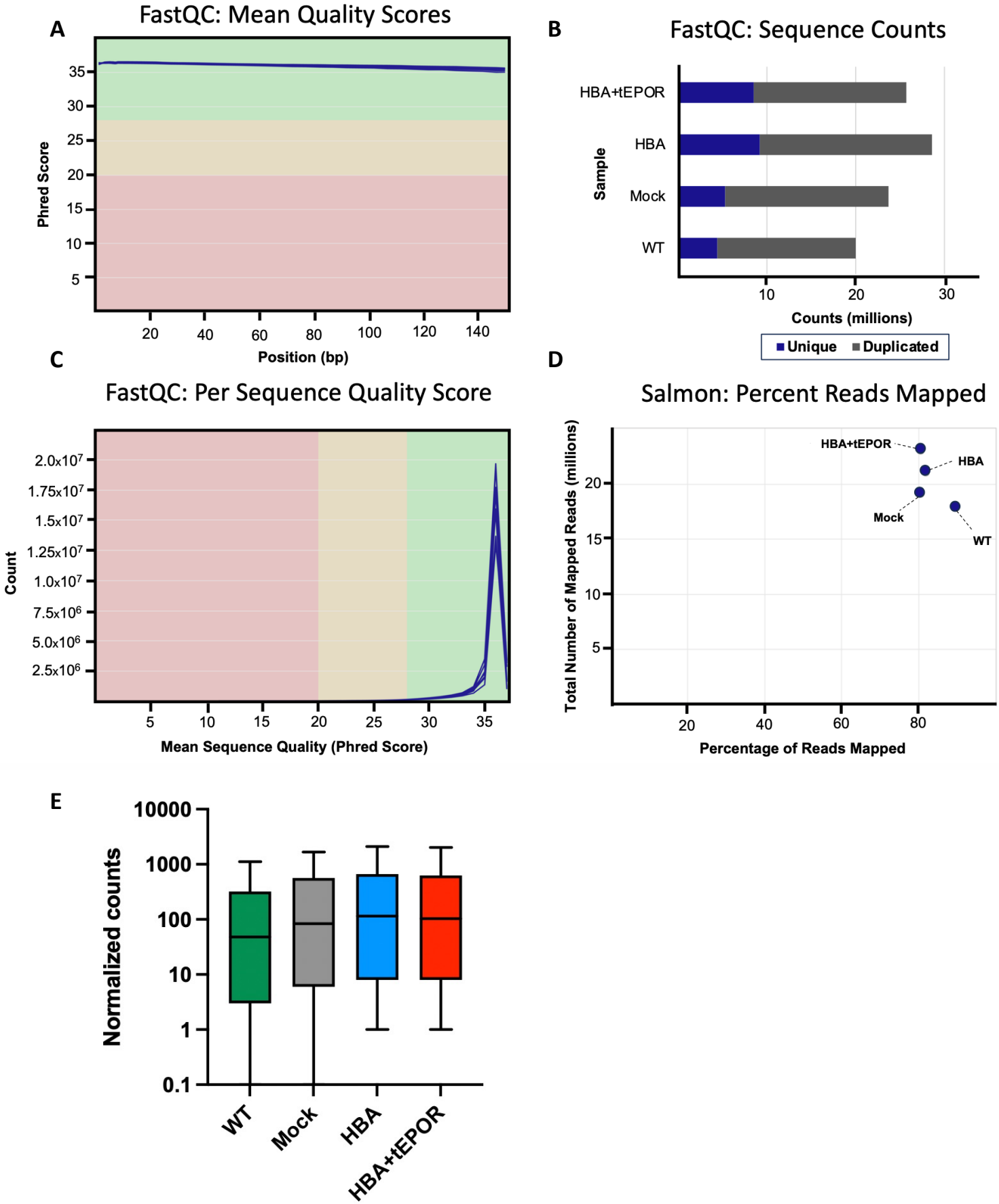
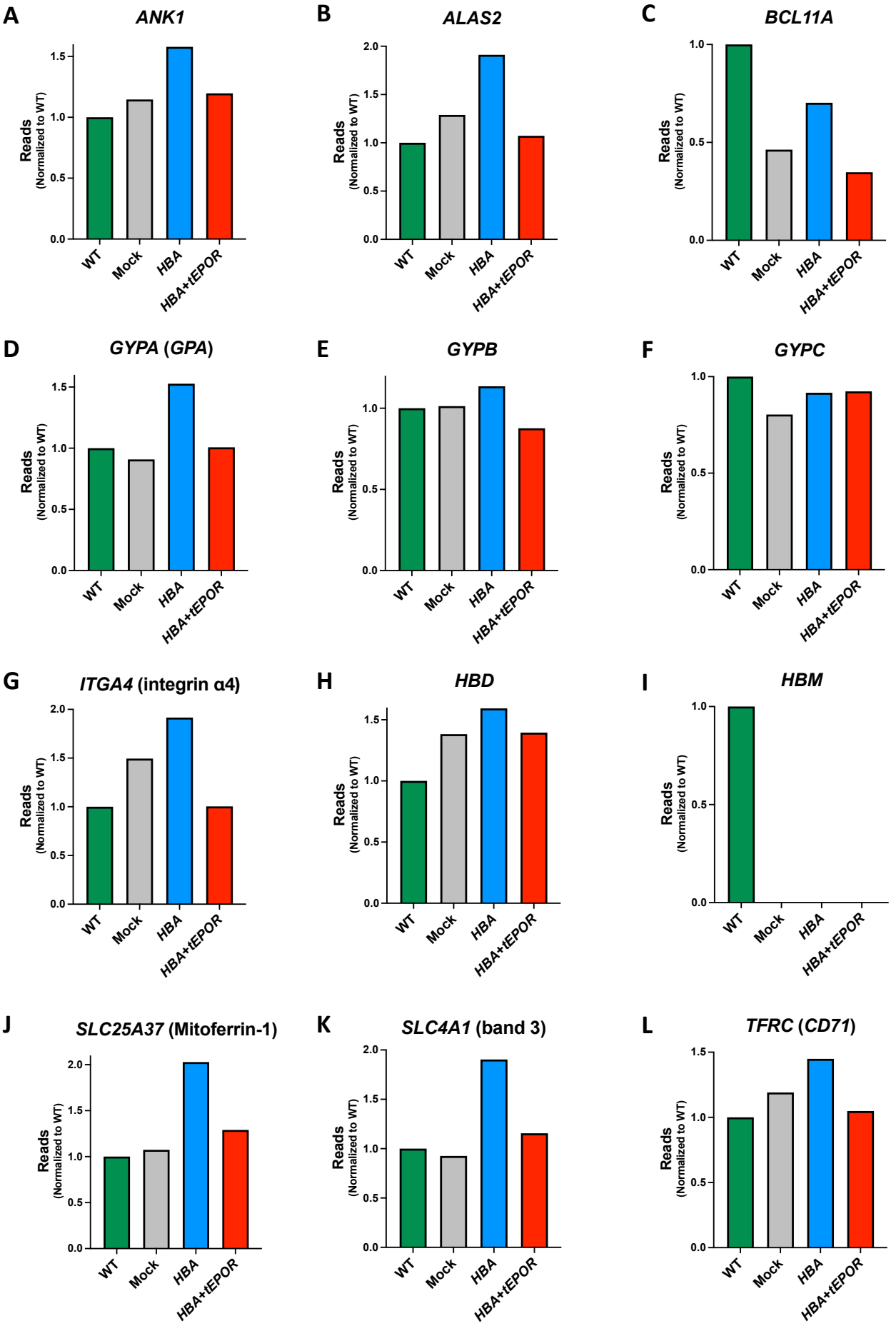
Supplemental Figure 6